International Journal of Molecular Sciences
International Journal of Molecular Sciences

*Article*

# Anticancer and antiphytopathogenic activity of fluorinated isatins and their water-soluble hydrazone derivatives

**Andrei Bogdanov [1,*,†], Margarita ~~Neganova~~[*,1] Neganova[1,2,*,†], Alexandra Voloshina [1], Anna Lyubina [1], Syumbelya Amerhanova [1], Igor Litvinov [1], Olga Tsivileva [3], Nurgali Akylbekov [4], Rakhmetulla Zhapparbergenov[4,*], Zulfiia Valiullina[5], Alexander Samorodov [5] and Igor Alabugin[1,6]**

[1] Arbuzov Institute of Organic and Physical Chemistry, FRC Kazan Scientific Center, Russian Academy of Sciences, Akad. Arbuzov st. 8, Kazan, 420088, Russia; abogdanov@inbox.ru (AB); microbi@iopc.ru (AV, AL, SA); litvinov@iopc.ru (IL); ialabugin@gmail.com (IA)
[2] Institute of Physiologically Active Compounds at Federal Research Center of Problems of Chemical Physics and Medicinal Chemistry, Russian Academy of Sciences, Severnij pr. 1, Chernogolovka, 142432, Russia
[3] Institute of Biochemistry and Physiology of Plants and Microorganisms, Saratov Scientific Centre of the Russian Academy of Sciences, Entuziastov ave. 13, Saratov, 410049, Russia; tsivileva_o@ibppm.ru (OT)
[4] Laboratory of Engineering Profile "Physical and Chemical Methods of Analysis", Korkyt Ata Kyzylorda University, Aitekebie str. 29A, Kyzylorda 120014, Kazakhstan; nurgali_089@mail.ru (NAk); ulagat-91@mail.ru (RZh)
[5] Bashkir State Medical University, Lenin st. 8, Ufa, 450008, Russia; z_suleimanova@mail.ru (ZV); avsamorodov@gmail.com (AS)
[6] Department of Chemistry and Biochemistry, Florida State University, 95 Chieftan Way, Tallahassee, FL 32306-4390, USA.

[†] - Contributed equally
* Correspondence: abogdanov@inbox.ru (AV), ulagat-91@mail.ru (R Zh), neganovam@ipac.ac.ru (MN), Tel.: +7-843-272-7384 (AV), +7-724-223-1041 (R Zh), +7-496-52-42-606 (MN)

**Abstract:** A series of new fluorinated 1-benzylisatins was synthesized in high yields via a simple one-pot procedure in order to explore the possible effect of ortho-fluoro- (**3a**), chloro- (**3b**), or bis-fluoro (**3d**) substitution on biological activity of this pharmacophore. Furthermore, the new isatins could be converted into water-soluble isatin-3-hydrazones using their acid-catalyzed reaction with Girard's reagent P and its dimethyl analogue. The cytotoxic action of these substances is associated with the induction of apoptosis caused by mitochondrial membrane dissipation and by stimulated reactive oxygen species production in tumor cells. In addition, compounds **3a** and **3b** exhibit platelet antiaggregation activity at the level of acetylsalicylic acid, and the whole series of fluorine-containing isatins does not adversely affect the hemostasis system as a whole. Among the new water-soluble pyridinium isatin-3-acylhydrazones, compounds **7c** and **5c,e** exhibit the highest antagonistic effect against phytopathogens of bacterial and fungal origin and can be considered as useful leads for combating plant diseases.

**Keywords:** isatin; quaternary ammonium compounds; cancer; hydrazones, crystal structure, antiphytopathogenes, cytotoxicity.

**Citation:** To be added by editorial staff during production.

Academic Editor: Firstname Lastname

Received: date
Accepted: date
Published: date

**Publisher's Note:** MDPI stays neutral with regard to jurisdictional claims in published maps and institutional affiliations.

**Copyright:** © 2023 by the authors. Submitted for possible open access publication under the terms and con-

## 1. Introduction

The isatin heterocyclic system is the precursor of a large number of derivatives [1, 2] with a wide range of biological and pharmacological properties [3-6]. A number of properties reported for this class of compounds include anticonvulsant [7, 8], antistress and

Formatted: Font: (Asian) DengXian, Bold
Formatted: Font: (Asian) DengXian, Bold
Style Definition: MDPI_3.7_itemize
Style Definition: MDPI_3.8_bullet
Style Definition: MDPI_7.1_References
Style Definition: MDPI_7.1_FootNotes
Style Definition: RSC R02 References
Formatted: English (United States)
Formatted: English (United States)
Formatted: Hyperlink
Formatted: Hyperlink
Formatted: English (United States)
Formatted: English (United States)
Formatted: Hyperlink
Formatted: Font: (Asian) DengXian

ditions of the Creative Commons At
tribution (CC BY) license (https://cr
ativecommons.org/licenses/by/4.0/).

anxiogenic [9], antiviral [10], antimicrobial [11], antituberculous [12], antimalarial [13], antifungal [14], and antibacterial [15], which determine their main areas of use. Among the many pharmacological or medical applications of isatin and its derivatives (Fig. 1), their use as antitumor agents deserves special attention. Several isatin derivatives have already passed clinical trials and become approved anticancer drugs [16]. In particular, the most promising isatin derivative, sunitinib, has been clinically approved by the FDA for the treatment of gastrointestinal stromal tumors, renal cell carcinoma, and a rare type of pancreatic cancer [17]. However, efforts are continuing to diversify chemical modifications and achieve deeper insights into the mechanism of biological action of isatin derivatives. Further rational research is needed to create more effective drugs with less systemic toxicity, better pharmacological characteristics and a clear mechanism of action.

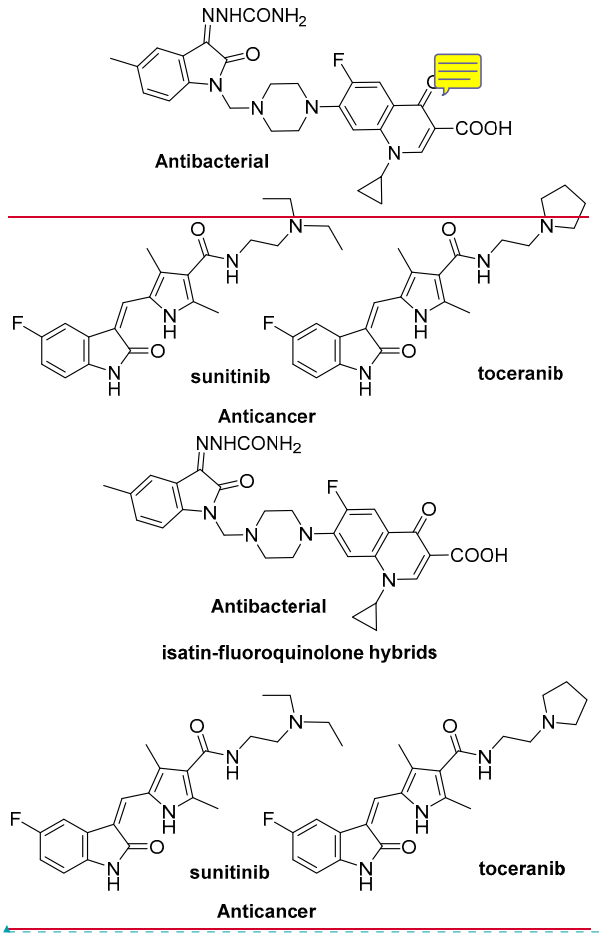


**Figure 1.** Fluorinated isatin derivatives exhibiting various types of biological activity

One of the limiting factors in the medical and biological applications of many isatin derivatives is their low water solubility. One approach to solving this problem is based on the introduction of an ammonium moiety. Not only does this positively charged group improve the desired physicochemical characteristics but it also can expand the range of

Field Code Changed

action of the compounds. This is evidenced by recent reviews on the therapeutic possibilities of various quaternary ammonium compounds [18-22]. Earlier, we have also demonstrated the high potential of isatin hydrazones containing a quaternary ammonium center in the search for drug candidates for combating human and plant diseases [23-27] (Fig. 2).

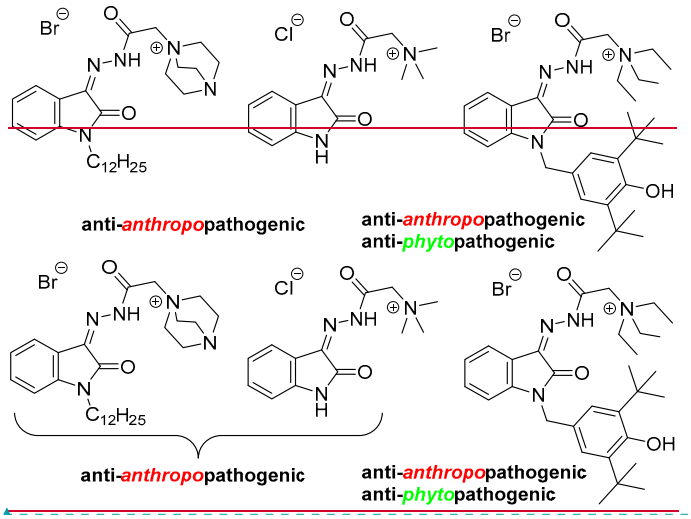


Field Code Changed

**Figure 2.** Isatin-3-acylhydrazones possessing antimicrobial activity

Another advantage of isatins as a promising platform for the design and development of new drugs is the possibility of introducing additional substituents at positions of the isatin ring. One of the popular approaches to chemical modifications is introduction of halogen atoms. For example, approximately 25–30% of new drugs at the market contain at least one fluorine atom [28]. This modification often leads to a significant increase in an existing type of biological activity and (or) expansion of the action spectrum [29].

In this work, we present novel fluorinated 1-benzylisatins and water-soluble hydrazones as a platform for the search for potential antitumor and antiphytopathogenic compounds.

## 2. Results and Discussion

### *2.1. Chemistry*

#### 2.1.1. Synthesis of diversely fluorinated 1-benzylisatins

Fluoro-substituted derivatives **3a-f** were synthesized by alkylation of 5-fluoro-isatin sodium salt **2** with halogen-containing benzyl halides (Scheme 1). Isatins **3a,c,e,f** contained only F-substituents but in different substitution patterns. In addition, we have prepared a mono-chloro isatin **3b** and a mixed 2-chloro-6-fluoro derivative **3d** in order to assess the contribution of the fluorine atom in the pendant benzene ring to the biological activity,

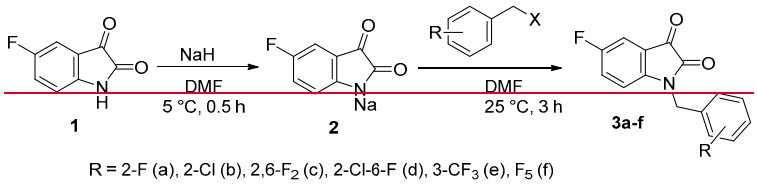


R = 2-F (a), 2-Cl (b), 2,6-$F_2$ (c), 2-Cl-6-F (d), 3-$CF_3$ (e), $F_5$ (f)

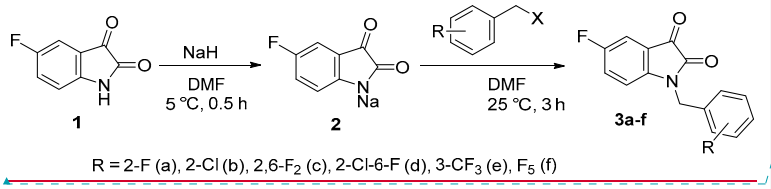


**Scheme 1.** Two-step one-pot synthesis of polyfluorinated 1-benzylisatins

The halogenated isatins **3a-f** were isolated in high yields in pure form immediately after work-up of the reaction mixtures. Their structure and purity have been unequivocally proven by IR and NMR spectroscopy and elemental analysis data (Figures S3-S56, Supplementary materials).

To further assess the effect of the position of the fluorine atom and the electronic structure of substituents in the benzyl fragment on the level of antitumor activity, a small series of derivatives **4a-e** was obtained by analogy (Scheme 2). In contrast to reactions described in Scheme 1, the alkylation of sodium salt **2** by less electrophilic benzylic halides requires heating in order to achieve higher yields of the target compounds.

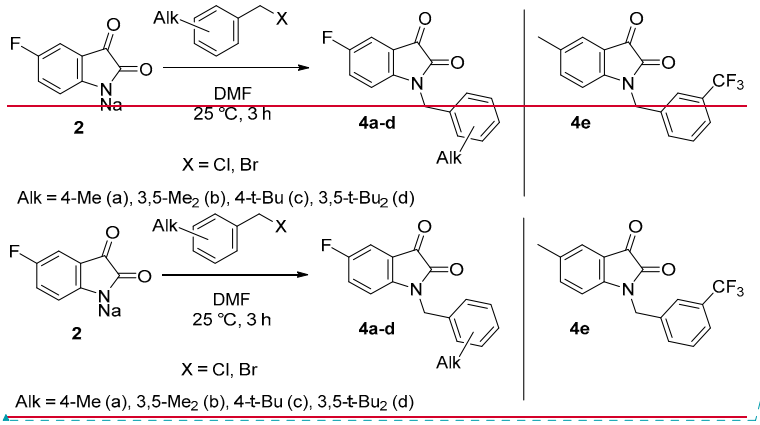


**Scheme 2.** Synthesis of 5-fluorinated 1-alkylbenzylisatins

In continuation of our research on the synthesis and biological activity of water-soluble isatin-3-acylhydrazones [for example, see 23-26], we also synthesized several new pyridinium acylhydrazones **5a-e,** and previously published more lipophilic analogues **7a-c** [26] (Fig. 43) containing fluorine atoms in various molecular fragments (Scheme 3).

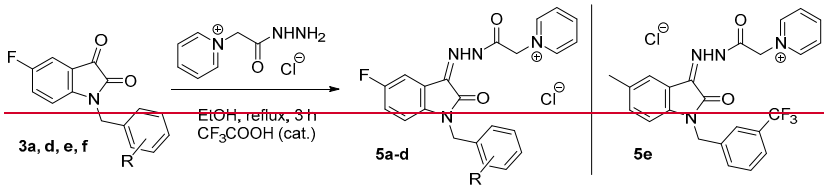


Field Code Changed

Field Code Changed

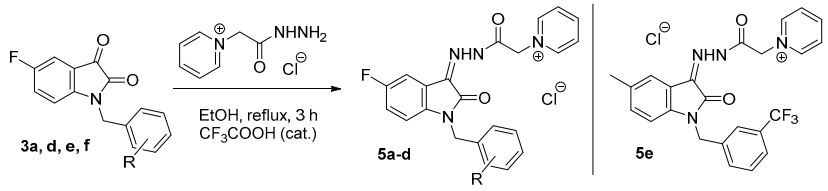


**Scheme 3.** Synthesis of fluorine-containing pyridinium isatin hydrazones

Compounds **5a-e** and **7a-c** were isolated in high yields (72-90%) after spontaneous cooling of the reaction mixture. They are yellow powders, soluble in water, aqueous DMSO and DMF but insoluble in non-polar solvents, ethanol, chloroform, etc. ~~For comparison, the pyridinium salts described by us earlier were used in the work [26] (Fig. 3).~~

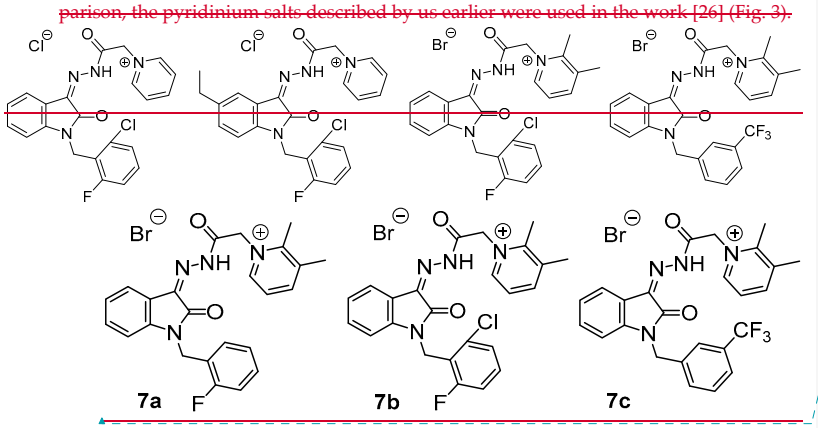


**Figure 3.** Previously published [26] ~~antimicrobial~~ fluorinated ~~isatin hydrazones~~

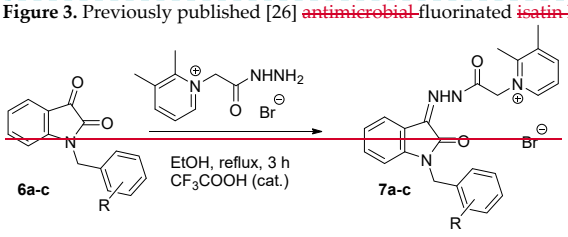


~~**Figure 4. Previously published [26]** dimethylpyridinium **salts under investigation** isatin~~ hydrazones

2.1.2. X-Ray study

According to X-Ray data (Figures ~~5a~~1a, b, Table S1) compounds **3f** and **4c** crystallize in different orthorhombic space groups: compound **3f** crystallizes in the non-centrosymmetric racemic space group *Pna2*$_1$, compound **4c** crystallizes in the centrosymmetric space group *Pbca*.

The conformations of the molecules in the crystals are similar: the isatin fragments are planar and the nitrogen atom N1 has planar trigonal coordination as typical for amides. The benzyl substituents at the nitrogen atom are positioned non-symmetrically along the N–C8 and C8–C9 bonds. Torsion angles C2-N1-C8-C9 and N1-C8-C9-C10(C14) in the molecule are **3f** -110.3(5) and -114.0(5)°, while in the molecule **4c**, they are -109.5(2) and -

Field Code Changed

Field Code Changed

**Formatted:** Centered, Indent: Left: 4.5 cm, First line: 0 cm

132.4(2)° respectively. This arrangement places one of the hydrogen atoms at the C8 atom in a nearly eclipsed conformation with the plane of the pendant benzene ring. In this case, the main geometric parameters (bond lengths and bond angles) in molecules **3f** and **4c** are usual.

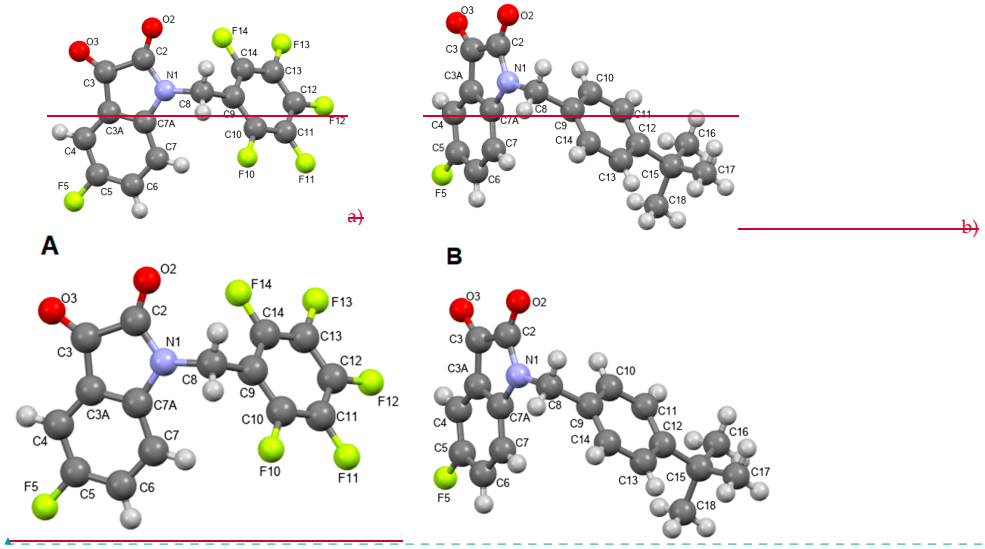


**Figure 5.** X-ray geometry of fluorinated isatins **3f** (A) and **4c** (B) in the crystals. Ellipsoids are shown with 50% probability.

Analysis of short contacts in crystals shows multiple C-H…F intermolecular contacts, contributing to crystal packing for these compounds. Such contacts can be considered as non-conventional H-bonds [30]. This observation suggests that the C-F bonds may participate in similar supramolecular interactions with their biological targets.

Thus, using simple and efficient synthetic procedures, we obtained various fluorine-containing oxindole derivatives, which can be divided into two main groups: isatins and isatin-3-hydrazones. In the next step, we proceeded to studies of their biological activity.

### 2.2. Biological Studies

Various modifications of isatin molecules can lead to the appearance of different desired properties. For example, phosphate derivatives of isatin hydrazones have been shown to have higher activity against the sugar cane phytopathogenic fungi *Colletotrichum falcatum*, *Fusarium oxysporum*, and *Curvularia pallescence* than some currently used synthetic fungicides [31]. Evaluation of the fungicidal activity of dialkylphosphorylhydrazones showed that several compounds are able to effectively inhibit growth of *Rhizoctonia solani* and *Fusarium oxysporum*. In addition, these compounds did not interfere with the germination of lettuce seeds, which indicates the absence of phytotoxicity and makes them potential leaders in the search for new fungicides [32].

Therefore, in studies of biological properties in this work, we approached from two main angles - for substituted isatins, we evaluated the potential of using these substances as antitumor drugs, and for pyridinium hydrazones, we assessed their prospects as antiphytopathogenic agents (Fig. 5).

Formatted Table

Formatted: Font color: Auto, Snap to grid

Formatted: Font color: Auto, Snap to grid

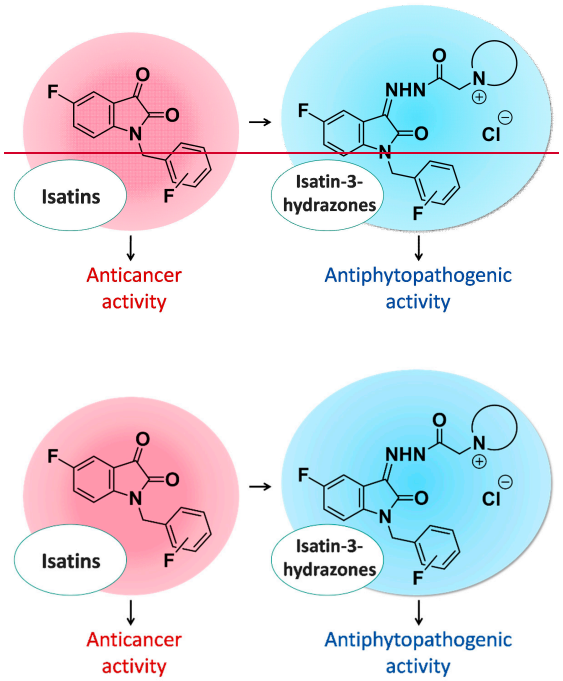


**Figure ~~6~~5.** Different biological activity profile of fluorinated isatin derivatives.

Formatted: rynqvb, Font color: Auto, Check spelling and grammar

2.2.1. Anticancer activity

The antitumor potential of the isatin derivatives synthesized in this work (**3a–6c**) and previously obtained (**8a–8d**) [26] (Fig. ~~7~~6) was primarily assessed by the ability of the compounds to reduce the survival rate of M-HeLa and HuTu 80 tumor-derived cells relative to that for the normal (Chang liver) cells. Further, in order to understand the possible mechanisms of the cytotoxic action of the most promising substances, the ability to induce apoptosis and Reactive Oxygen Species (ROS) production was also determined, as well as the anticoagulant and antiaggregation properties were studied.

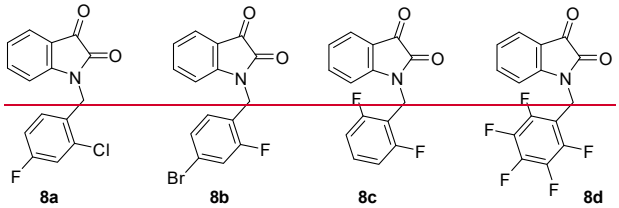

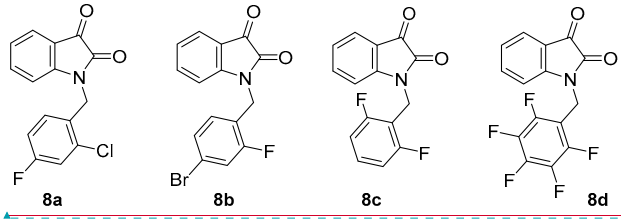


**Figure ~~7~~6.** Previously published fluoroisatins under investigation

2.2.1.1 – Cytotoxicity of test compounds

The toxic effect of all test compounds on cancer and normal cells was evaluated. The cytotoxicity of synthesized isatins was compared with the currently used antitumor ~~drugs tamoxifen (TAM) and~~drug 5-fluorouracil (5-FU) [33]. ~~The $IC_{50}$ parameter was calculated using the AAT Bioquest program [34].~~

Table 1. Cytotoxic activity ($IC_{50}$) and selectivity (SI) of synthesized isatins~~.~~*.

| Compd | $IC_{50}$ (μM) | | |
|---|---|---|---|
| | Cancer cell line | | Normal cell line |
| | [a]M-HeLa | [b]HuTu 80 | [c]Chang liver |
| **3a** | 74.6±5.9 | 25.2±1.9 (*SI ~ 2.1*) | 53.0±4.2 |
| **3b** | 32.1±2.5 (*SI ~ 2.2*) | 38.3±3.0 (*SI ~ 1.8*) | 71.5±5.6 |
| **3c** | 65.7±5.9 | 41.2±2.7 | 95.5±8.0 |
| **3d** | 53.8±4.3 (*SI ~ 1.9*) | 31.0±2.4 (*SI ~ 3.2*) | >100 |
| **3f** | 100±7.4 | 92.0±6.4 | >100 |
| **4a** | 44.7±3.3 | 44.0±2.9 | 80.0±5.8 |
| **4b** | 58.8±4.4 | 50.0±3.8 | 63.2±5.5 |
| **4c** | >100 | 43.0±3.0 | 92.1±7.4 |
| **4d** | 58.4±4.1 | 33.3±2.3 | 39.4±2.8 |
| **4e** | 94.0±7.5 | 53.2±3.9 | >100 |
| **6a** | 98.0±6.8 | 100±8.4 | 76.1±5.3 |
| **6b** | 44.4±3.2 | 37.6±2.6 | 76.0±5.4 |
| **6c** | 83.0±5.7 | 59.4±4.2 | >100 |
| **8a** | 50.0±3.7 | 64.0±4.5 | >100 |
| **8b** | 40.0±2.8 | 59.4±4.2 | 100±8.4 |
| **8c** | 98.8±6.9 | 50.3±3.6 | 79.0±5.5 |
| **8d** | >100 | 54.1±3.9 | >100 |
| ~~TAM~~ | ~~28.0±2.5 (*SI ~ 1.7*)~~ | ~~n.a.~~ | ~~46.2±3.5~~ |
| 5-FU | 62.0±4.9 | 65.2±5.6 | 19.0±1.7 |

* The incubation time was 24 h; [a]M-HeLa — human cervical epithelioid carcinoma cell lines; [b]HuTu-80 — human duodenal adenocarcinoma cell lines; [c]Chang liver – normal human hepatocyte; ~~TAM – tamoxifen,~~ 5-FU – 5-fluorouracil; n.a. – non-active. Experiments were carried out in triplicate.

All test compounds exhibit moderate activity against the cancer lines used in the experiments in conjunction with moderate to low cytotoxicity against the normal human liver cell line, i.e. the Chang liver cells (Table 1). Compounds **3a**, **3b**, and **3d**, containing

Field Code Changed

Formatted: Russian

Formatted Table

Formatted Table

an ortho-substituted benzyl fragment with fluorine (**3a**), chlorine (**3b**), or both (**3d**) atoms, have the highest activity against both tumor cell lines. It should be noted that for substance **3b**, the cytotoxicity is 2.0 times higher than the activity of the reference drug 5-FU.

The selectivity of compounds for cancer cells is an important criterion for evaluating a potential drug. ~~To evaluate it, the selectivity index (SI) is calculated as the ratio between the $IC_{50}$ for normal cells and the $IC_{50}$ for cancer cells [35].~~ The calculated selectivity values (SI) for the most active compounds were 2.2 for M-HeLa for **3b**, 1.9 for **3d**~~, 1.7 for TAM, and <1 for the rest~~; HuTu-80 for **3a** - 2.1, **3b** - 1.8, for **3d** - 3.2, for 5-FU <1. The selectivity values (SI) indicated in the table prove that the halogenated isatins exhibit greater selectivity than the reference drugs ~~TAM and~~ 5-FU.

2.2.1.2 – Apoptosis

It is well known that tumor cells are able to avoid apoptosis, which leads to uncontrolled abnormal proliferation and rapid tumor growth. Substances capable of inducing apoptotic death in tumor cells are promising agents in the fight against cancer [~~36~~34]. Flow cytometry (Guava easy Cyte, MERCK, USA) showed that the most cytotoxic compounds **3a**, **3b**, and **3d** were able to induce apoptosis in HuTu-80 cells. Figure ~~8~~7 shows the apoptotic effects induced by the selected substances at $IC_{50}/2$ and $IC_{50}$ cytotoxicity concentrations.

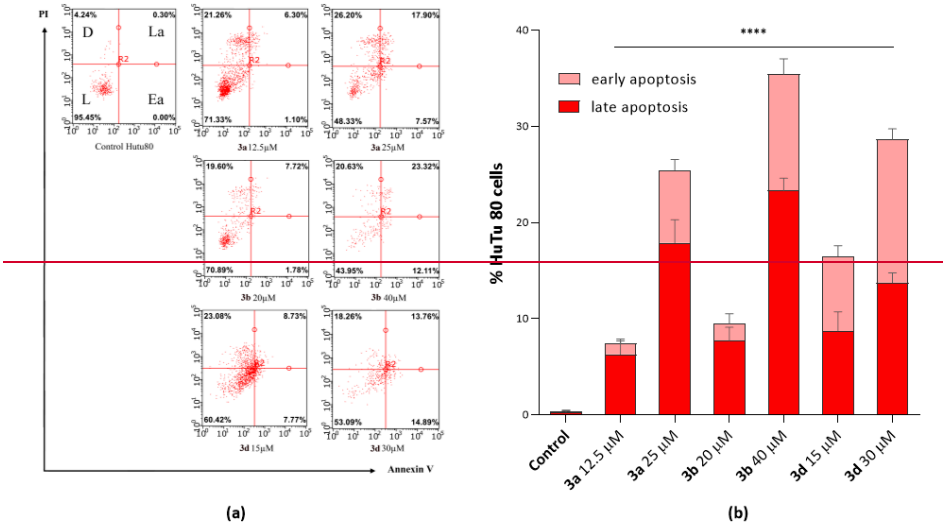

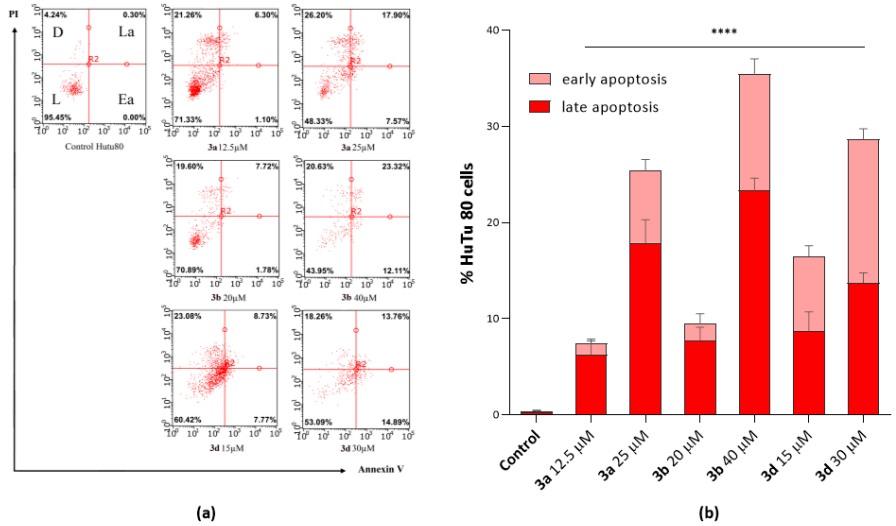


**Figure** ~~8~~7. Apoptosis induction in HuTu 80 cells incubated with compounds **3a**, **3b**, and **3d** at $IC_{50}/2$ and $IC_{50}$ concentrations. Values are presented as mean ± standard deviation (in triplicate), L - live cells; D - dead cells; Ea - cells in early apoptosis; La - cells in late apoptosis. **** - p <0.0001 versus Control. The statistical analysis was performed using two-way ANOVA and the Bonferroni test.

It can be seen from the presented data that after 24-hour incubation of HuTu 80 cells with compounds **3a**, **3b**, and **3d**, the number of cells at both the early and late stages of apoptosis increase with concentration. Molecule **3b** exhibits the highest apoptosis-inducing activity ($IC_{50}$ concentration of 40 μM). Moreover, in the presence of these compounds, cells exist predominantly in the stage of late apoptosis.

2.2.1.3 – Mitochondrial membrane potential

Apoptosis can be triggered via two main pathways, o which is closely related to mitochondria. The normal functioning of these organelles depends on the potential and permeability of the mitochondrial membrane. Disturbance of these characteristics leads to the release of proapoptotic factors into the cell cytosol, caspase cascade activation, and initiation of internal mitochondrial pathway of apoptosis. To analyze the effect of compounds **3a**, **3b**, and **3d** on changes in the mitochondrial membrane potential, we performed flow cytometry using JC-10 fluorescent dye (in the Mitochondria Membrane Potential Kit). In normal cells (with high membrane potential), JC-10 accumulates in the mitochondrial matrix, where it forms aggregates with red fluorescence. However, in apoptotic cells, JC-10 diffuses out of mitochondria, converts to its monomeric form, and emits green fluorescence, which is recorded by a flow cytometer [~~37~~35]. As can be seen in Figure ~~9~~8, after a 24-hour incubation of HuTu 80 cells with the tested substances, a decrease in the mitochondrial membrane potential is observed, which becomes more pronounced at concentrations corresponding to the $IC_{50}$ values of cytotoxicity. Compounds **3b** and **3d** showed the highest activity in this test, under the action of which the green fluorescence increases up to 55% relative to the control.

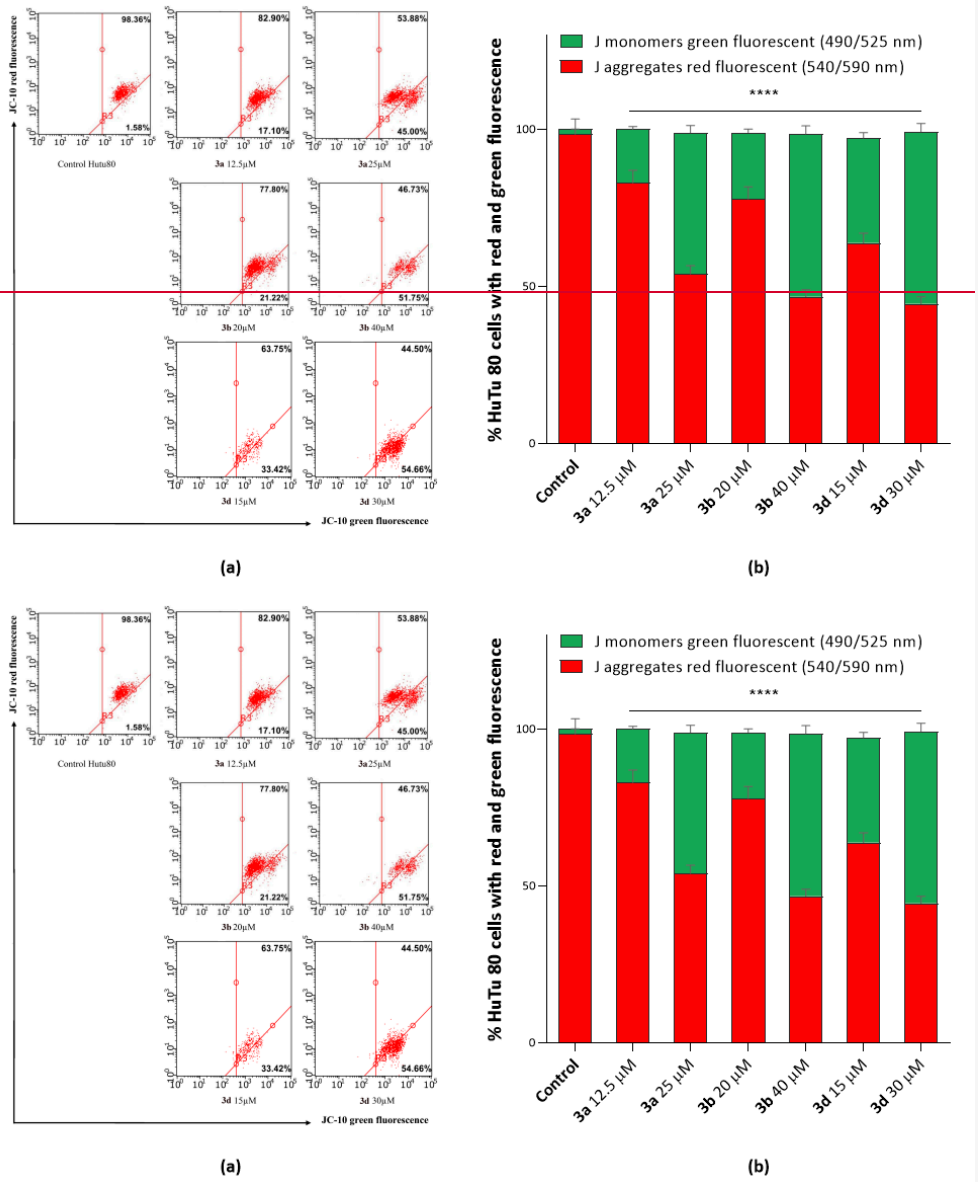




(a)
(b)


**Figure ~~98~~.** (a) Effects of compounds **3a**, **3b**, and **3d** on mitochondrial membrane potential. (b) Quantitative distribution of HuTu 80 cells in % with red aggregates and green monomers. **** - p <0.0001 versus Control. The statistical analysis was performed using two-way ANOVA and the Bonferroni test.

Thus, these results confirm that the mechanism of action of compounds **3a**, **3b**, and **3d** is associated with the induction of apoptosis, which occurs along the internal mitochondrial pathway due to the ability of substances to dissipate the mitochondrial membrane.

2.2.1.4 – Reactive oxygen species production

An increase in the production of reactive oxygen species (ROS) by the halogenated isatins is another characteristic feature for the development of apoptosis along the mitochondrial pathway. Mitochondria are both a potential source and a target of ROS. ROS are known to lead to disruption of mitochondrial functions and, consequently, to irreversible cell damage [~~38~~36].

We have evaluated the effect of compounds **3a**, **3b**, and **3d** in HuTu 80 cells on the induction of ROS production using a flow cytometry assay and the CellROX® Deep Red flow cytometry kit. The results are presented in Fig. ~~10~~9.

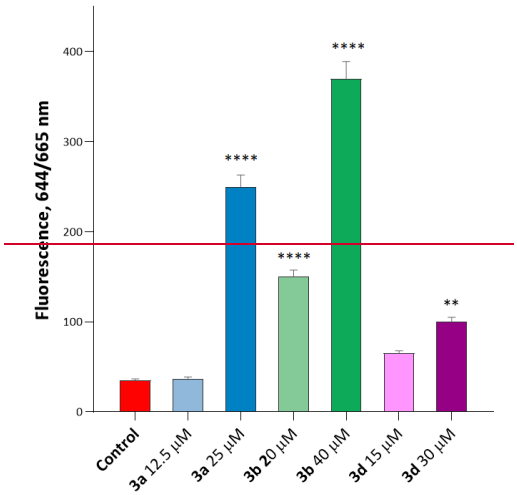

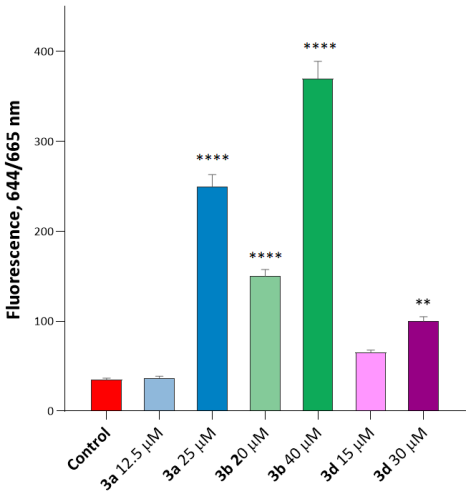


**Figure ~~10~~9.** Induction of ROS production by compounds **3a**, **3b**, and **3d**

The data show a significant dose-dependent increase in CellROX® Deep Red fluorescence intensity for compounds **3a** and **3b**. Interestingly, compound **3a** showed only small (1.1-fold) increase in ROS production at 12.5 μM (below its $IC_{50}$), but the ROS production increas[illegible]7.1 times relative to the control at 25 μM. This indicates a significant dose-dependent increase in ROS production in the presence of this substance. Other substituted isatins **3b** and **3d** led to increased ROS production relative to the control. ** - p ≤ 0.01 and **** - p <0.0001 versus Control. The statistical analysis was performed using one-way ANOVA and the Dunnet test.

2.2.1.5 – Anticoagulant and Anti-aggregation Activities Study

In numerous systematic reviews and meta-analyses, there is a large amount of evidence that excessive platelet count contributes to the progression of malignant neoplasms [37-~~39~~~~41~~]. This is due to the formation of specific interactions between platelets and neoplastic cells, which leads to increased survival of tumor cells in the bloodstream, increased spread of tumor foci and, as a result, metastasis in places remote from the primary occurrence [~~42~~40]. In addition, the metastatic growth of a malignant neoplasm may be due to disturbances in epigenetic regulation - an increased level of oncoproteins and hypersecretion of tumor growth factors - caused precisely as a result of the pathology of platelet signaling pathways. Thus, an increase in platelet count directly correlates with unfavorable prognosis in patients with lung [~~43~~41], prostate [~~44 48~~42-46], etc. [~~49~~47] carcinoma, protecting tumor cells from recognition by the immune system and, as a result, elimination. Thus, patients with an abnormally high platelet count represent a phenomenal clinical problem due to the ineffectiveness of using existing approaches for their therapy. In this regard, considerable attention of researchers is focused on the use of the well-known anticoagulant, acetylsalicylic acid (aspirin), as an adjunctive therapy for oncological diseases, which is an irreversible inhibitor of platelet cyclooxygenase [~~50~~48], and a number of clinical studies have demonstrated its positive clinical effects in the treatment of prostate cancer [~~51~~49] and mammary glands [~~52~~50], stomach [~~53~~51], etc. That is why the presence of antiplatelet properties as a mechanism of action of potential antitumor agents is considered as a promising approach to the development of therapeutic agents to combat oncopathologies.

In this work, for the three most promising compounds **3a**, **3b** and **3d**, anticoagulant and antiaggregation properties were studied (Table 2).

**Table 2.** Anticoagulant and antiaggregation activity of compounds **3a, 3b** and **3d.**

| Cmpd | Latent period, % of control | Maximum amplitude (MA), % of control | Aggregation rate, % of control | Time to MA, % of control | APTT[$], % of control |
|---|---|---|---|---|---|
| **3a** | +12.3 (11.7-14.5)*, †, # | -11.8 (9.4–14.3)*, † | -12.7 (10.8–15.7)*, † | -8.7 (7.6–10.8)*,†, # | +11.2 (9.5-13.7)* |
| **3b** | +10.3 (7.3-11.8)*, †, # | -15.3 (13.9-17.2)*, † | -16.8 (14.6-19.1)*,†,# | +9.3 (8.7-11.4)*,† | +8.3 (6.4-9.1)* |
| **3d** | +2.4 (1.3-2.7)†,# | -8.2 (6.1-10.5)*,†,# | -15.7 (11.9-17.6)*,† | +17.5(16.4-18.7)*,† | +6.2(4.7-10.3)* |
| **Acetylsalicylic acid** | -2.1 (1.1–2.6)† | -13.7 (10.8-16.4)*, † | -10.5 (7.6-12.3)*, † | +10.5 (8.7-13.4)*, † | - |
| **Heparin sodium** | - | - | - | - | +20.3 (19.7-21.4)* |

*p ≤ 0.05, **p ≤ 0.001 - compared to control; #p ≤ 0.05, ##p ≤ 0.001 - compared to acetylsalicylic acid; †p ≤ 0.05, ††p ≤ 0.001 - compared to Heparin sodium; [$] APTT - activated partial thromboplastin time.

Among the studied class of compounds, derivatives **3a** and **3b** showed antiaggregation activity at the level of acetylsalicylic acid, reducing the maximum platelet aggregation by 12% on average. At the same time, compounds **3a** and **3b**, in contrast to acetylsalicylic acid, lengthen the lag-period by more than 10% relative to the control. From the point of view of anticoagulant properties, all compounds, including **3d**, showed a different level of influence on the plasma component of the hemostasis system, which manifested itself in a change in only the indicator of the internal blood coagulation pathway - activated partial thromboplastin time (APTT).Thus, fluorine containing isatins and corresponding water-soluble acylhydrazones have high potential as a scaffold for the development of effective anticoagulant and antiaggregation agents.

Thus, the isatin derivatives synthesized in this work have the potential to be used as a basis for the design of antitumor agents with a known mechanism of action. The most cytotoxic compounds are capable of inducing the production and accumulation of reactive oxygen species, by disrupting the normal functioning of mitochondria and dissipating the mitochondrial membrane. These pathological processes, provoked by the action of substances, lead to the launch of a cascade of cell death along the internal pathway of apoptosis, which is directly associated with mitochondria.

2.2.2. Evaluation of antiphytopathogenic activity of water-soluble hydrazones

2.2.2.1 – Antibacterial activity

Complexation of several compounds with isatin was demonstrated to yield good antibacterial potentialities frequently based on the synergic effects of isatin combinations against selected microorganisms [~~54~~52]. The current list of bacterial pathogens isolated from various crop plants and commonly grown vegetables frequently comprises *Micrococcus luteus*, *Pseudomonas fluorescens*, *Pectobacterium carotovorum* (*Erwinia carotovora*), *Xanthomonas campestris*, and *Pectobacterium atrosepticum* (*Erwinia carotovora* subsp. *atrosepticum*) [53-55~~-57~~]. The top five cereal bacterial pathogens list includes *Pseudomonas* and *Xanthomonas* [~~58~~56]. The species of *Pseudomonas* genus are found in soil, water, on plant organs and around the roots of plants. *Pseudomonas fluorescens* is ~~an~~a ubiquitous opportunistic bacterium that inhabits all major freshwater, marine and terrestrial ecosystems. Moreover, the species of *Ps. fluorescens* are frequently encountered in hospitals as a contaminant of

Formatted Table

injectable material and surfaces [~~59, 60~~57, 58]. Species of Gram-negative short rod-shaped aerobic bacteria from the *Xanthomonas* genus include a wide range of plant pathogens that cause numerous and diverse diseases in all kinds of plant genera [~~61~~59]. Gram-positive bacterial species *Micrococcus luteus* widely distributed in the environment along with Gram-negative pathogenic species *Pectobacterium carotovorum* subsp. *carotovorum* cause various bacterial infections [~~62~~60]. Besides, the species of potato-associated rhizosphere bacterium *Pectobacterium atrosepticum* are known as causative agent of a soft rot infection in potato tubers [~~63~~61]. Hence, nowadays greater efforts are needed to find new antimicrobial agents.

We examined the synthesized isatin derivatives for their antibacterial effects against the above test organisms. Along with the solutions of **5a-e, 7a-c**, test compounds were sodium hypochlorite (1000 μg/ml), chlorohexidin (500 μg/ml), and norfloxacin (500 μg/ml), a synthetic fluoroquinolone with broad-spectrum antibacterial activity against most bacteria [~~64~~62]. The in vitro bactericidal activity of the target compounds **5a-e, 7a-c** against five representative phytopathogens is summarized in the Table S2.

The results showed the bactericidal activity distinct from zero against *M. luteus* B-109, *P. atrosepticum* 1043, *P. carotovorum* subsp. *carotovorum* MI, *Ps. fluorescens* EL-2.1, *X. campestris* B-610 for all the compounds tested.

Compounds **5a**, **5b**, **5d**, **7a** containing 2-fluorobenzyl- (**5a**, **7a**), 6-chloro-2-fluorobenzyl- (**5b**), or (perfluorophenyl)methyl- (**5d**) substituents at 1 position of 2-oxoindolin (**7a**) or 5-fluoro-2-oxoindolin (**5a**, **5b**, **5d**) moiety of their molecules showed moderate bactericidal activity (Table S2).

Even though four compounds **5a**, **5b**, **5d**, **7a** demonstrated non-zero bactericidal action, however, there were worse results in **7a** when affecting *M. luteus*, and in **5b**, **5d** vs *X. campestris*, the inhibition zone width being less than 3 mm. Higher antibacterial potential was revealed for the hydrazone **7a** ~~(Table 2.2.2)~~ with broader spectrum against *P. carotovorum* subsp. *carotovorum* MI, *Ps. fluorescens* EL-2.1, and *X. campestris* B-610, as well as wider inhibition zone (5-6 mm).

Compounds **5c**, **5e**, **7b**, **7c** could be arranged into a group exhibiting a more potent ability to combat bacterial pathogens under study (Table S3, Fig. ~~11~~10).

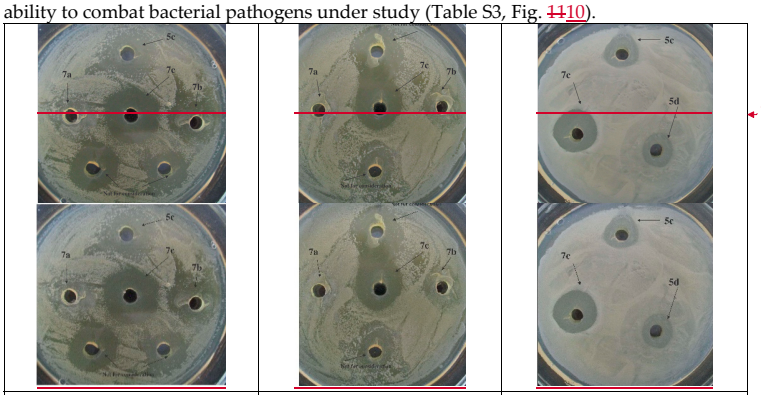


| a | b | c |
|---|---|---|

**Figure ~~11~~10.** Bactericidal action of compounds tested against *X. campestris* B-610 (a), *Pseudomonas fluorescens* EL-2.1 (b), *P. carotovorum* subsp. *carotovorum* MI (c)

Structural peculiarity of the compounds **7a**, **7b**, **7c** is that they are 2,3-dimethylpyridin-1-ium salts, whereas all other hydrazones (**5a**, **5b**, **5c**, **5d**, **5e**) are pyridin-1-ium salts. However, the substances **5c**, **5e**, and **7b,** with distinctly structured pyridinium fragment, displayed virtually the same bactericidal effect assessed by the inhibition zone range of 4 to 7 mm dependent to the test system used (Table S3).

**Formatted:** Font: Italic

**Formatted Table**

Greater antibacterial activity by the given hydrazone seems to be connected to the presence of trifluoromethyl group on phenyl ring in the side-chain substituent. Trifluoromethylated compounds are of utmost interest due to their unique properties including the in vitro antifungal activity [~~65~~63]. However, a few previous works reported that the complicated structured trifluoro derivatives of indole displayed minimal antifungal activity against *Fusaruim*, with the inhibition rate about 73% at as high concentration as 500 mcg/ml [~~66~~64]. In our work, it was the compound **7c** containing 3-trifluoromethylbenzyl substituent at 1 position of 2-oxoindolin moiety, that shows the best-in-experiment bactericidal activity. Other hydrazones from this group, **5c**, **5e**, **7b**, displayed a slightly diminished bactericidal effect and formed a 5-mm to 7-mm zone of the pathogens' growth inhibition (Table S3).

Taking into account the data on the values of the inhibition zone width (mm~~) (Table 2.2.1~~), it is conditionally possible to arrange the studied 2 mM solutions of compounds **5a-e, 7a-c** in descending order of activity as follows: **7c** (6–9 mm) > **5e** (4–7 mm) ≈ **5c** (4–7mm) ≈ **7b** (4–7 mm) > **5a** (3–6 mm) > **7a** (2–6 mm) > **5b** (2,5–4 mm) > **5d** (2–4 mm). Thus, with respect to the phytopathogens used, the most profound activity was shown by the hydrazone **7c**.

Formatted: English (United Kingdom)

2.2.2.2 – Antifungal activity

Fungal pathogens cause 70–80% of all plant diseases [~~67~~65], possessing a potentiality of causing large-scale disease outbreaks in a very limited period of time. Among the diverse mycelial pathogenic fungi, those from the genera *Fusarium* and *Phytophthora* are among of the most destructive plant pathogens known, have broad host ranges, and are capable of causing crop losses. Damage from these pathogens results in the destruction of the roots until the entire plant dies, and in an eventual collapse of whole infected plants [~~68~~66]. The trans-kingdom pathogen *Fusarium oxysporum* is referred to as aggressive among *Fusarium* species causing devastating plant vascular wilt diseases. In particular, different branches of food industry are extremely conscious of *Fusarium* infections of cereals [~~69~~67]. *F. oxysporum* species complex includes both plant and human pathogens that cause threaten public health [~~70~~68]. *Phytophthora cactorum* is a causative agent of phytophthora blight of ginseng (*Panax ginseng*), a plant, which is very useful for conventional medicine to treat a variety of diseases including cancer [~~71~~69]. Therefore, search for novel antifungal agents has been a constant hot research topic in pesticide development, especially because a long-term usage of the same antifungal agent often leads to an increase in the resistance of phytopathogenic fungi [~~72~~70].

In this study, a series of fluorine-containing pyridinium isatin hydrazones **5a-e, 7a-c** was prepared, and their antifungal activities were evaluated. The mycelial growth rate method was used to determine the inhibitory effect of these compounds at serial concentration gradient on the mycelial growth of *F. oxysporum* and *P. cactorum*. Along with the solutions of hydrazones, test compounds were fludioxonil and N-cetylpyridinium chloride. These commercial widely used fungicides capable of inhibiting the pathogenic fungi mycelium propagation served for the purpose of comparison in the course of the fungicidal effect assays. Fludioxonil is one of the most potent fungicides against the diseases of agricultural crops caused by the representatives of both *Fusarium* spp. and *Phytophthora* spp. [~~73~~71]. Under laboratory conditions, the assessment of the phytopathogenic fungi resistance to fludioxonil is conducted at its concentrations from 0.1 to 10 μg/mL [~~74~~72]. N-cetylpyridinium chloride (CPC) is a quaternary ammonium compound with the broad-spectrum antimicrobial activity [~~75~~73] used in topical formulations with antifungal activity [~~76, 77~~74, 75].

Screening for antifungal properties of the compounds **5a-e, 7a-c** introduced into the agar medium for fungal culture *F. oxysporum* and *P. cactorum* was carried out in the concentration range of 1 to 50 nanomol/ml, that was equivalent to the mass/volume concentration about 0.5 to 22 μg/mL. The extent of fungal growth inhibition was expressed as a percentage, taking into account that the quantitative characteristic of the absence of inhibition is expressed as 0%. The half maximal effective concentration $EC_{50}$ was calculated

using the dependence of *C* as the concentration of the compound or standard antibiotic, on *I* as inhibition of radial growth of the colony relative to the non-fungicidal control. The method is based on the approach related to the proper dependence between dose (it is *C*) and response (it is *I*) under the assumption of "control" as "zero inhibition". The linear approximation of this dependence fits the equation, from which a target $EC_{50}$ value is calculated at $I = 50$ [~~78, 79~~76, 77].

The in vitro antifungal activity of target compounds **5a-e, 7a-c** against the fungal pathogen *F. oxysporum* is summarized in Table S4.

Within the entire experiment with the phytopathogen *F. oxysporum*, the highest fungicidal activity estimated through the $EC_{50}$ indices (μg/mL) was displayed by the studied compounds **5e** (0.60) and **7a** (7.25). Antifungal activity of the rest hydrazones tested was also considerable with the $EC_{50}$ value not exceeding 21 μg/mL for **7b**. The methyl group at C5 position of oxindole moiety in combination with the trifluoromethyl group on the benzyl ring (**5e**) of the 1-benzylisatin hydrazones, as well as the fluorine atom at C2 position on this benzyl ring (**7a**), had a significant effect on the pyridinium isatin hydrazones antifungal activity against *F. oxysporum* (Fig. ~~12~~11).

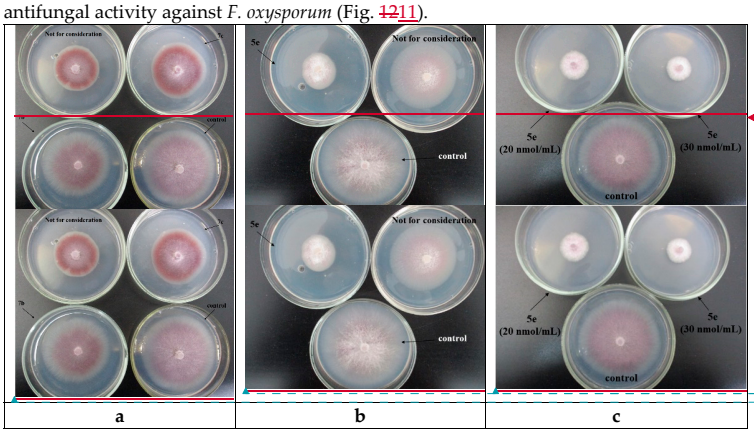


**Figure ~~12~~11.** Growth of *Fusarium oxysporum* IBPPM 543 on agar media fortified with the compounds **7c** and **7b** (C 20 nmol/mL (a); **5e** (C 3 nmol/mL) (b); **5e** (C 20 and 30 nmol/mL) (c).

Compound **5e** had the most significant antifungal activity against *F. oxysporum* ($IC_{50}$ = 0.60 μg/mL).

The in vitro antifungal activity of target compounds **5a-e, 7a-c** against the fungal pathogen *P. cactorum* is summarized in the Table S5.

Within the entire experiment with the phytopathogen *P. cactorum*, the highest fungicidal activity assessed through the $EC_{50}$ parameter (μg/mL) was displayed by the studied compounds **5a** (15.12), **5c** (15.40), and **5b** (18.19). Antifungal activity of the rest of the tested hydrazones was also considerable with the $EC_{50}$ value not exceeding 28 μg/mL for **7b**. The fluorine atom (**5a**, **5b**, **5c**) at C5 position of the isatin skeleton in the pyridinium isatin hydrazones in combination with the strong electron-withdrawing units: trifluoromethyl group ($-CF_3$) (**5c**), or fluorine atom at C2 position (**5a**), or 2-Cl-6-F (**5b**) substituent, on the benzyl ring of the 1-benzylisatin hydrazones, had a significant effect on the improvement of the antimicrobial activity against *P. cactorum*. Compounds **5a** and **5c** exhibited essentially the same antifungal activity equal to 15 μg/mL.

All of the fluorine-containing compounds **5a-e, 7a-c** showed an antagonistic effect against the oomycete *P. cactorum*. This effect is somewhat superior to that of N-cetylpyridinium chloride by 1.3 (**5e**, **7b**) to 2.3 (**5a**, **5c**) times, and of fludioxonil by 1.1 (**5e**, **7b**) to 2.0 (**5a**) times in 5 days of the *Phytophthora* growth. At the same culture age of ascomycete *F. oxysporum*, all of the studied fluorine-containing compounds outperformed the reference fungicides in the antifungal effect in this test-system. Fludioxonil was less efficient than

Formatted Table

**Formatted:** html-italic, Check spelling and grammar

**Formatted:** html-italic, Check spelling and grammar

**Formatted:** html-italic, Check spelling and grammar

hydrazones in inhibiting the *Fusarium* growth. Inhibition by hydrazon ranged from by 139 times than **5e** down to 4.1 times than **7b**. N-cetylpyridinium chloride showed a weaker fungicidal action vs *F. oxysporum*, as compared to **5a-e, 7a-c**, by 235 times than **5e** down to 7.0 times than **7b**.

When comparing the fungicidal activity of hydrazones in the *F. oxysporum* test system and their antagonistic action with respect to *P. cactorum*, one can recognized that, without exceptions, all compounds under study show the greater ability to inhibit the mycelial propagation of *F. oxysporum* (Table 3).

**Table 3.** Comparative fungicidal activity of hydrazones **5a-e, 7a-c** against *Fusarium oxysporum* IBPPM 543 and *Phytophthora cactorum* VKM F-985

| Соединение | $EC_{50}$, μg/mL* at day 5 | |
|---|---|---|
| | *F. oxysporum* | *P. cactorum* |
| **5a** | 13.84 | 15.12 |
| **5b** | 14.84 | 18.19 |
| **5c** | 14.92 | 15.40 |
| **5d** | 17.35 | 24.74 |
| **5e** | 0.60 | 27.43 |
| **7a** | 7.25 | 22.87 |
| **7b** | 20.24 | 27.51 |
| **7c** | 13.90 | 19.98 |
| Fludioxonil | 83.33 | 29.51 |
| N-cetylpyridinium chloride | 141.1 | 34.79 |

* the average values are given; the standard deviation did not exceed 0.03 from the given value.

The inhibiting action of fluorine-containing hydrazones **5a-e, 7a-c** judged through the $EC_{50}$ criterion occurred to be stronger with respect to *Fusarium* mycelial development, by 46 times than **5e** down to 1.1 times than **5c**, in comparison to the same compounds' impact on *Phytophthora*. In contrast, the reference fungicides exhibited the opposite tendency for the fungal test-system used. Fludioxonil and N-cetylpyridinium chloride showed much greater effect of *P. cactorum* growth inhibition compared to *F. oxysporum* (2.8 and 4.1 times, respectively, for two fungicides in Table 3). The behavior of the fluorine-free compounds synthesized and examined for antiphytopathogenic activity by us earlier [25] was in line with the latter tendency, i.e., they were similar to the reference fungicides. The results could testify to a promising synthetic strategy potentially resulting in the fluorine-containing hydrazones uncommonly efficient vs. *Fusarium oxysporum* in comparison with known fungicides.

## 3. Materials and Methods

### *3.1. Chemistry*

IR spectra were recorded on IR Fourier spectrometer Tensor 37 (Bruker Optik GmbH, Germany) in the 400–3600 $cm^{-1}$ range in KBr. The $^1$H-, $^{19}$F-, and $^{13}$C-NMR spectra were recorded on a Bruker AVANCE 400 spectrometer (Bruker BioSpin, Rheinstetten, Germany) operating at 400 MHz (for $^1$H NMR), 377 MHz (for $^{19}$F NMR) and 101 MHz (for $^{13}$C NMR), Brucker spectrometers AVANCE*III*-500 (Bruker BioSpin, Rheinstetten, Germany) operating at 500 MHz (for $^1$H NMR) and 126 MHz (for $^{13}$C MMR) and Bruker Avance 600 spectrometer (Bruker BioSpin, Rheinstetten, Germany) operating at 600 MHz (for $^1$H NMR) and 151 MHz (for $^{13}$C NMR). Chemical shifts were measured in δ (ppm) with reference to the solvent (δ = 7.27 ppm and 77.00 ppm for $CDCl_3$, δ = 2.50 ppm and 39.50 ppm for DMSO-$d_6$, for $^1$H and $^{13}$C NMR, respectively). Elemental analysis was performed on a CHNS-O Elemental Analyser EuroEA3028-HT-OM (EuroVector S.p.A., Milan, Italy). The melting points were determined on Stuart SMP10 apparatus (Birmingham, UK).

Formatted Table

**X-ray crystallography data.** Data of **3f** and **4c** were collected on a Bruker D8 QUEST with PHOTON II CCD diffractometer (Bruker AXS, Germany), using graphite monochromated MoKα ($\lambda$ = 0.71073 Å) radiation and ω-scan rotation. Data collection images were indexed, integrated, and scaled using the APEX3 [~~80~~78] data reduction ~~package[79]~~package and corrected for absorption using SADABS [~~81~~79]. The structure was solved by direct methods and refined using SHELX program [~~82~~80]. All non-hydrogen atoms were refined anisotropically. H atoms were calculated on idealized positions and refined as riding atoms. Crystal Data and Refinement Details are presented in Table S1 (see SM). The X-ray analysis was performed on the equipment of Spectral-Analytical Center of FRC Kazan Scientific Center of RAS.

CCDC 2268269, 2268273 (**3f** and **4c**) contain the supplementary crystallographic data for this paper. These data can be obtained free of charge via www.ccdc.cam.ac.uk/conts/retrieving.html or from the Cambridge Crystallographic Data Centre, 12 Union Road, Cambridge CB2 1EZ, UK; fax: (+44) 1223-336-033; or deposit@ccdc.cam.uk).

**Synthesis of fluorine-containing indolin-2,3-diones (isatins) 3a-f, 4a-e (general method).** To a magnetically stirred solution of 5-substituted isatin **1** (10 mmol) in dry DMF (20 ml) NaH (10 mmol, 60% suspension in mineral oil) was added in portions during 30 min at 5°C (ice-water external bath). During the addition of sodium hydride, the reaction mixture turns purple. After 30 min, the corresponding benzyl halide (10 mmol) was added ~~to a dark violet reaction mixture~~ dropwise, followed by additional stirring at r.t. (3 h for **3a-f,** 6 h for **4a-e**). Then, a solution was poured into an ice/water mixture (w/w 100 g/200 g), the precipitate that formed was filtered off, washed consecutively with cold water (50 ml), light petroleum (40 ml) and dried in vacuo~~.~~ (12 Torr). For better precipitation of the target product in the case of alkylbenzyl isatins, sodium chloride (10 g) was added to the mixture of ice and water.

**5-Fluoro-1-(2-fluorobenzyl)indoline-2,3-dione (3a)**. Orange powder. Yield 95%, m.p. = 120-121 °C. IR spectrum, ν, $cm^{-1}$: 1333 (C-F), 1621 (C=C), 1732 (C=O), 3066 (CH). $^1$H NMR (600 MHz, $CDCl_3$) δ 7.37-7.28 (m, 3H, Ph), 7.26-7.21 (m, 1H, Ar), 7.15-7.08 (m, 2H, Ar), 6.88 (dd, *J* = 8.6 Hz, *J* = 3.6 Hz, 1H, Ar), 4.97 (s, 2H, $CH_2$). $^{13}$C NMR (151 MHz, $CDCl_3$) δ 182.4, 160.8 (d, *J* = 176.9 Hz, C-F), 159.2 (d, *J* = 176.5 Hz, C-F), 158.1, 146.5, 130.3 (d, *J* = 8.1 Hz, C-F, CH), 130.0 (d, *J* = 1.8 Hz, C-F, CH), 124.9 (d, *J* = 2.4 Hz, C-F, CH), 124.8 (d, *J* = 24.2 Hz, C-F, CH), 121.4 (d, *J* = 14.3 Hz, C-F), 118.3 (d, *J* = 6.9 Hz, C-F), 115.8 (d, *J* = 21.6 Hz, C-F, CH), 112.4 (d, *J* = 24.3 Hz, C-F, CH), 111.9 (d, *J* = 3.1 Hz, C-F, CH), 37.4 (d, *J* = 4.0 Hz, C-F, $CH_2$). ). $^{19}$F NMR (600 MHz, DMSO-$d_6$) δ -119.9, -119.5. Found: C, 65.87; H, 3.34; F, 13.83; N, 5.11. Anal. calcd (%) for $C_{15}H_9F_2NO_2$: C, 65.94; H, 3.32; F, 13.91; N, 5.13.

**1-(2-Chlorobenzyl)-5-fluoroindoline-2,3-dione (3b)**. Light orange powder. Yield 76%, m.p. = 167-168 °C. IR spectrum, ν, $cm^{-1}$: 746 (CCl), 1344 (C-F), 1620 (C=C), 1733 (C=O), 3061 (CH). $^1$H NMR (500 MHz, $CDCl_3$) δ 7.43 (d, 1H, *J* = 7.4 Hz, Ar), 7.34 (dd, *J* = 6.5 Hz, *J* = 2.7 Hz, 1H, Ar), 7.29-7.19 (m, 4H, Ar), 6.74 (dd, *J* = 8.6 Hz, *J* = 3.5 Hz, 1H, Ar), 5.06 (s, 2H, $CH_2$). $^{13}$C NMR (126 MHz, DMSO-$d_6$) δ 182.1 (d, *J* = 1.6 Hz, C-F), 158.6 (d, *J* = 241.2 Hz, C-F), 158.5, 146.4, 132.2 (CH), 131.8, 129.4 (d, *J* = 22.8 Hz, C-F, CH), 128.3 (CH), 127.4 (CH), 123.9, 123.7, 118.9 (d, *J* = 7.0 Hz, C-F), 112.2 (d, *J* = 7.6 Hz, C-F, CH), 111.5 (d, *J* = 24.4 Hz, C-F, CH), 41.2 ($CH_2$). $^{19}$F NMR (600 MHz, DMSO-$d_6$) δ -119.8. Found: C, 62.21; H, 3.15; Cl, 12.19; F, 6.46; N, 4.78. Anal. calcd (%) for $C_{15}H_9ClFNO_2$: C, 62.19; H, 3.13; Cl, 12.24; F, 6.56; N, 4.84.

**1-(2,6-Difluorobenzyl)-5-fluoroindoline-2,3-dione (3c)**. Red powder. Yield 85%, m.p. 131-132 °C. IR spectrum, ν, $cm^{-1}$: 1327 (C-F), 1623 (C=C), 1735 (C=O), 1753 (C=O), 3057 (CH). $^1$H NMR (500 MHz, $CDCl_3$) δ 7.34-7.28 (m, 2H, Ar), 7.24 (ddd, *J* = 8.8 Hz, *J* = 8.7 Hz, *J* = 2.7 Hz, 1H, Ar), 6.94 (dd, *J* = 8.1 Hz, *J* = 8.0 Hz, 1H, Ar), 6.88 (dd, *J* = 8.7 Hz, *J* = 3.6 Hz, 1H, Ar), 5.02 (s, 2H, $CH_2$). $^{13}$C NMR (126 MHz, $CDCl_3$) δ 182.3, 161.5 (dd, $^1J$ = 250.4 Hz, $^3J$ = 7.3 Hz, C-F), 159.3 (d, *J* = 246.1 Hz, C-F), 157.3 (d, *J* = 0.6 Hz, C-F), 146.3 (d, *J* = 2.0 Hz), 130.7 (t, *J* = 10.4 Hz, C-F, CH), 124.7 (d, *J* = 24.2 Hz, C-F, CH), 118.4 (d, *J* = 7.0 Hz, C-F), 112.4 (dd, *J* = 24.2 Hz, *J* = 0.3 Hz, C-F, CH), 111.8 (dd, *J* = 25.1 Hz, *J* = 6.1 Hz, C-F, CH), 111.5 (dt, *J* = 9.2 Hz, *J* = 2.4 Hz, C-F, CH), 109.9 (t, *J* = 18.2 Hz, C-F), 32.3 (t, *J* = 4.0 Hz, C-F, $CH_2$). Found:

**Formatted:** Font color: Black

C, 61.80; H, 2.80; F, 19.45; N, 4.77. Anal. calcd (%) for $C_{15}H_8F_3NO_2$: C, 61.86; H, 2.77; F, 19.57; N, 4.81.

**1-(2-Chloro-6-fluorobenzyl)-5-fluoroindoline-2,3-dione (3d)**. Bright orange powder. Yield 90%, m.p. = 140-141 °C. IR spectrum, ν, $cm^{-1}$: 779 (CCl), 1330 (C-F), 1624 (C=C), 1745 (C=O), 1772 (C=O), 3070 (CH). $^1$H NMR (500 MHz, $CDCl_3$) δ 7.32-7.27 (m, 3H, Ar), 7.20 (ddd, *J* = 8.7 Hz, *J* = 8.7 Hz, *J* = 2.7 Hz, 1H, Ar), 7.07-7.02 (m, 1H, Ar), 6.80 (dd, *J* = 8.7 Hz, *J* = 3.6 Hz, 1H, Ar), 5.12 (d, *J* = 0.8 Hz, 2H, $CH_2$). $^{13}$C NMR (126 MHz, DMSO-*d*$_6$) δ 182.2 (d, *J* = 0.7 Hz, C-F), 161.4 (d, *J* = 249.7 Hz, C-F), 158.4 (d, *J* = 241.6 Hz, C-F), 157.8, 146.8, 134.3 (d, *J* = 5.3 Hz, C-F, CH), 130.9 (d, *J* = 10.0 Hz, C-F), 125.9 (d, *J* = 2.9 Hz, C-F, CH), 124.3 (d, *J* = 24.2 Hz, C-F, CH), 120.3 (d, *J* = 16.4 Hz, C-F), 118.5 (d, *J* = 7.4 Hz, C-F), 114.9 (d, *J* = 22.5 Hz, C-F, CH), 112.0 (d, *J* = 6.3 Hz, C-F, CH), 111.6 (d, *J* = 24.4 Hz, C-F, CH), 36.2 (d, *J* = 3.2 Hz, C-F, $CH_2$). $^{19}$F NMR (600 MHz, DMSO-*d*$_6$) δ -119.8, -111.0. Found: C, 58.60; H, 2.59; Cl, 11.48; F, 12.23; N, 4.54. Anal. calcd (%) for $C_{15}H_8ClF_2NO_2$: C, 58.56; H, 2.62; Cl, 11.52; F, 12.35; N, 4.55.

**5-Fluoro-1-(3-(trifluoromethyl)benzyl)indoline-2,3-dione (3e)**. Orange powder. Yield 83%, m.p. = 170-171 °C. IR spectrum, ν, $cm^{-1}$: 1330 (C-F), 1621 (C=C), 1731 (C=O), 1745 (C=O), 3066 (CH). $^1$H NMR (400 MHz, DMSO-*d*$_6$) δ 7.85 (s, 1H, Ar), 7.75 (d, *J* = 7.7 Hz, 1H, Ar), 7.65 (d, *J* = 7.8 Hz, 1H, Ar), 7.58 (t, *J* = 7.7 Hz, 1H, Ar), 7.49 (dd, *J* = 7.2 Hz, *J* = 2.7 Hz, 1H, Ar), 7.45 (ddd, *J* = 9.3 Hz, *J* = 8.8 Hz, *J* = 2.8 Hz, 1H, Ar), 6.98 (dd, *J* = 8.6 Hz, *J* = 3.8 Hz, 1H, Ar), 5.01 (s, 2H, $CH_2$). $^{13}$C NMR (101 MHz, DMSO-*d*$_6$) δ 182.2, 158.5 (d, *J* = 241.3 Hz, C-F), 158.6, 146.2, 137.0, 131.4 (CH), 129.7 (CH), 129.3 (q, *J* = 31.6 Hz, C-F), 124.3 (m, CH), 124.1 (m, CH), 123.6 (d, *J* = 24.1 Hz, C-F, CH), 118.9 (d, *J* = 7.3 Hz, C-F), 112.1 (d, *J* = 7.6 Hz, C-F, CH), 111.5 (d, *J* = 22.4 Hz, C-F, CH), 42.5 ($CH_2$). Found: C, 59.40; H, 2.83; F, 23.47; N, 4.30. Anal. calcd (%) for $C_{16}H_9F_4NO_2$: C, 59.45; H, 2.81; F, 23.51; N, 4.33.

**5-Fluoro-1-((perfluorophenyl)methyl)indoline-2,3-dione (3f)**. Purple powder. Yield 75%, m.p. = 112-113 °C. IR spectrum, ν, $cm^{-1}$: 1330 (C-F), 1625 (C=C), 1749 (C=O), 3054 (CH). $^1$H NMR (500 MHz, $CDCl_3$) δ 7.37-7.30 (m, 2H, Ar), 6.89 (dd, *J* = 8.6 Hz, *J* = 3.4 Hz, 1H, Ar), 5.04 (s, 2H, $CH_2$). $^{13}$C NMR (126 MHz, $CDCl_3$) δ 181.5 (d, *J* = 1.8 Hz, C-F), 159.5 (d, *J* = 247.1 Hz, C-F), 157.3, 151.9-149.3 (m, C-F), 146.8-144.3 (m, C-F), 145.6 (d, *J* = 1.7 Hz, C-F), 142.9-140.4 (m, C-F), 136.8-136.2 (m, C-F), 124.9 (d, *J* = 24.3 Hz, C-F, CH), 118.5 (d, *J* = 6.9 Hz, C-F), 112.8 (d, *J* = 24.3 Hz, C-F, CH), 111.1 (d, *J* = 7.1 Hz, C-F, CH), 32.1 ($CH_2$). Found: C, 52.13; H, 1.56; F, 32.93; N, 4.00. Anal. calcd (%) for $C_{15}H_5F_6NO_2$: C, 52.19; H, 1.46; F, 33.02; N, 4.06.

**5-Fluoro-1-(4-methylbenzyl)indoline-2,3-dione (4a).** Orange powder. Yield 73%, m.p. = 111-112 °C. IR spectrum, ν, $cm^{-1}$: 1330 (C-F), 1623 (C=C), 1730 (C=O), 1741 (C=O), 2923 (CH). $^1$H NMR (500 MHz, DMSO-*d*$_6$) δ 7.48-7.41 (m, 2H, Ar), 7.31 (d, *J* = 8.0 Hz, 1H, Ar), 7.14 (d, *J* = 7.9 Hz, 1H, Ar), 6.95 (dd, *J* = 8.6 Hz, *J* = 3.8 Hz, 1H, Ar), 4.86 (s, 2H, $CH_2$), 2.27 (s, 3H, $CH_3$). $^{13}$C NMR (126 MHz, DMSO-*d*$_6$) δ 182.5 (d, *J* = 2.0 Hz, C-F), 158.5 (d, *J* = 241.3 Hz, C-F), 158.3, 146.5 (d, *J* = 1.4 Hz, C-F), 136.7, 132.2, 129.2 (CH), 127.3 (CH), 123.8 (d, *J* = 24.2 Hz, C-F, CH), 118.6 (d, *J* = 7.3 Hz, C-F), 112.4 (d, *J* = 7.4 Hz, C-F, CH), 111.4 (d, *J* = 24.4 Hz, C-F, CH), 42.7 ($CH_2$), 20.6 ($CH_3$). Found: C, 71.29; H, 4.43; F, 7.00; N, 5.16. Anal. calcd (%) for $C_{16}H_{12}FNO_2$: C, 71.37; H, 4.49; F, 7.06; N, 5.20.

**1-(3,5-Dimethylbenzyl)-5-fluoroindoline-2,3-dione (4b).** Light orange powder. Yield 70%, m.p. = 97-98 °C. IR spectrum, ν, $cm^{-1}$: 1341 (C-F), 1623 (C=C), 1741 (C=O), 2922 (CH). $^1$H NMR (400 MHz, $CDCl_3$) δ 7.30 (dd, *J* = 6.5 Hz, *J* = 2.7 Hz, 1H, Ar), 7.20 (ddd, *J* = 8.6 Hz, *J* = 8.6 Hz, *J* = 2.7 Hz, 1H, Ar), 6.93 (s, 1H, Ar), 6.91 (s, 2H, Ar), 6.75 (dd, *J* = 8.6 Hz, *J* = 3.6 Hz, 1H, Ar), 4.84 (s, 2H, $CH_2$), 2.28 (s, 6H, $CH_3$). $^{13}$C NMR (101 MHz, $CDCl_3$) δ 182.8 (d, *J* = 1.7 Hz, C-F), 159.3 (d, *J* = 246.0 Hz, C-F), 158.1, 146.9 (d, *J* = 1.7 Hz, C-F), 138.8, 134.0, 129.9 (CH), 125.1 (CH), 124.6 (d, *J* = 24.1 Hz, C-F, CH), 118.3 (d, *J* = 7.0 Hz, C-F), 112.4 (d, *J* = 15.3 Hz, C-F, CH), 112.2 (d, *J* = 0.9 Hz, C-F, CH), 44.1 ($CH_2$), 21.2 ($CH_3$). Found: C, 72.00; H, 4.95; F, 6.60; N, 4.90. Anal. calcd (%) for $C_{17}H_{14}FNO_2$: C, 72.07; H, 4.98; F, 6.71; N, 4.94.

**1-(4-(*tert*-Butyl)benzyl)-5-fluoroindoline-2,3-dione (4c).** Orange powder. Yield 71%, m.p. = 123-124 °C. IR spectrum, ν, $cm^{-1}$: 1333 (C-F), 1623 (C=C), 1734 (C=O), 2959 (CH), 3063 (CH). $^1$H NMR (400 MHz, $CDCl_3$) δ 7.36 (d, *J* = 8.6 Hz, 2H, Ar), 7.29 (dd, *J* = 6.5 Hz, *J* = 2.7 Hz, 1H, Ar), 7.25 (d, *J* = 8.6 Hz, 2H, Ar), 7.20 (ddd, *J* = 8.7 Hz, *J* = 8.7 Hz, *J* = 2.7 Hz, 1H, Ar), 6.78 (dd, *J* = 8.6 Hz, *J* = 3.6 Hz, 1H, Ar), 4.89 (s, 2H, $CH_2$), 1.29 (s, 9H, $CH_3$). $^{13}$C

NMR (101 MHz, $CDCl_3$) δ 182.7 (d, *J* = 1.9 Hz, C-F), 159.3 (d, *J* = 245.9 Hz, C-F), 158.0, 151.4, 146.9 (d, *J* = 1.6 Hz, C-F), 131.1, 127.2 (CH), 126.0 (CH), 124.5 (d, *J* = 24.1 Hz, C-F, CH), 118.2 (d, *J* = 7.0 Hz, C-F), 112.4 (d, *J* = 12.6 Hz, C-F, CH), 112.2 (d, *J* = 4.4 Hz, C-F, CH), 43.8 ($CH_2$), 34.5, 31.2 ($CH_3$). Found: C, 73.21; H, 5.80; F, 6.01; N, 4.43. Anal. calcd (%) for $C_{19}H_{18}FNO_2$: C, 73.30; H, 5.83; F, 6.10; N, 4.50.

**1-(3,5-Di-*tert*-butylbenzyl)-5-fluoroindoline-2,3-dione (4d).** Orange powder. Yield 72%, m.p. = 136-137 °C. IR spectrum, ν, $cm^{-1}$: 1342 (C-F), 1622 (C=C), 1734 (C=O), 2964 (CH), 3043 (CH). $^1$H NMR (400 MHz, $CDCl_3$) δ 7.37 (s, 1H, Ar), 7.32 (dd, *J* = 6.4 Hz, *J* = 2.5 Hz, 1H, Ar), 7.21 (ddd, *J* = 8.6 Hz, *J* = 8.6 Hz, *J* = 2.4 Hz, 1H, Ar), 7.14 (s, 2H, Ar), 6.80 (dd, *J* = 8.6 Hz, *J* = 3.5 Hz, 1H, Ar), 4.90 (s, 2H, $CH_2$), 1.29 (s, 18H, $CH_3$). $^{13}$C NMR (101 MHz, $CDCl_3$) δ 182.8 (d, *J* = 1.9 Hz, C-F), 159.3 (d, *J* = 245.9 Hz, C-F), 158.1 (d, *J* = 1.0 Hz, C-F), 151.8, 147.1 (d, *J* = 1.7 Hz, C-F), 133.4, 124.4 (d, *J* = 24.1 Hz, C-F, CH), 122.2 (CH), 121.8 (CH), 118.3 (d, *J* = 7.0 Hz, C-F), 112.3 (d, *J* = 29.4 Hz, C-F, CH), 112.2 (CH), 44.8 ($CH_2$), 34.8, 31.4 ($CH_3$). Found: C, 75.15; H, 7.10; F, 5.09; N, 3.72. Anal. calcd (%) for $C_{23}H_{26}FNO_2$: C, 75.18; H, 7.13; F, 5.17; N, 3.81.

**5-Methyl-1-(3-(trifluoromethyl)benzyl)indoline-2,3-dione (4e).** Orange powder. Yield 86%, m.p. = 155-156 °C. IR spectrum, ν, $cm^{-1}$: 1329 (C-F), 1620 (C=C), 1728 (C=O), 1742 (C=O), 2929 (CH), 3035 (CH). $^1$H NMR (500 MHz, DMSO-$d_6$) δ 7.83 (s, 1H, Ar), 7.73 (d, *J* = 7.6 Hz, 1H, Ar), 7.64 (d, *J* = 7.8 Hz, 1H, Ar), 7.57 (dd, *J* = 7.7 Hz, *J* = 7.7 Hz, 1H, Ar), 7.40-7.38 (m, 2H, Ar), 6.88 (d, *J* = 8.7 Hz, 1H, Ar), 5.00 (s, 2H, $CH_2$), 2.26 (s, 3H, $CH_3$). $^{13}$C NMR (126 MHz, DMSO-$d_6$) δ 183.0, 158.5, 147.9, 138.1 (CH), 137.2, 132.7 (CH), 131.3 (CH), 129.6, 129.3 (q, *J* = 31.7 Hz, C-F), 124.7 (CH), 124.2 (q, *J* = 3.8 Hz, C-F, CH), 124.1 (q, *J* = 3.7 Hz, C-F, CH), 124.0 (q, *J* = 272.4 Hz, $CF_3$), 117.8, 110.6 (CH), 42.4 ($CH_2$), 20.0 ($CH_3$). Found: C, 63.87; H, 3.73; F, 17.80; N, 4.38. Anal. calcd (%) for $C_{17}H_{12}F_3NO_2$: C, 63.95; H, 3.79; F, 17.85; N, 4.39.

**Synthesis of fluorine-containing isatin-3-acylhydrazones 5~~,6~~ (general method).** To the mixture of substituted isatin (10 mmol) and 15 ml of absolute ethanol, Girard's reagent P (10 mmol) and three drops of trifluoroacetic acid were successively added. The reaction solution was heated under reflux for 3 h. After spontaneously cooling to room temperature, the precipitate formed was filtered, washed with absolute ether and dried in vacuum.

**1-(2-(2-(5-Fluoro-1-(2-fluorobenzyl)-2-oxoindolin-3-ylidene)hydrazinyl)-2-oxoethyl)pyridin-1-ium chloride (5a)**. Yellow powder. Yield 90%, m.p. = 180-182 °C. IR spectrum, ν, $cm^{-1}$: 1358 (C-F), 1621 (C=C), 1686 (C=O), 3017 (CH), 3391 (NH). $^1$H NMR (500 MHz, DMSO-$d_6$) δ 12.65 (s, 1H, NH), 9.23 (d, *J* = 5.2 Hz, 2H, Ar), 8.74 (t, *J* = 7.8 Hz, 1H, Ar), 8.28 (t, *J* = 6.9 Hz, 2H, Ar), 7.50 (d, *J* = 5.9 Hz, 1H, Ar), 7.42-7.30 (m, 3H, Ar), 7.25-7.16 (m, 2H, Ar), 7.12 (dd, *J* = 8.6 Hz, *J* = 3.9 Hz, 1H, Ar), 6.33 (s, 2H, $CH_2$). 4.93 (s, 2H, $CH_2$). $^{13}$C NMR (126 MHz, DMSO-$d_6$) δ 167.8, 160.9 (d, *J* = 246.0 Hz, C-F), 160.4, 158.8 (d, *J* = 239.6 Hz, C-F), 158.1, 146.6 (CH), 146.5 (CH), 146.2, 139.2, 130.0 (d, *J* = 7.9 Hz, C-F, CH), 129.8 (d, *J* = 3.3 Hz, C-F, CH), 127.7 (CH), 124.7 (d, *J* = 2.8 Hz, C-F, CH), 122.9 (d, *J* = 14.6 Hz, C-F), 120.3, 118.4 (d, *J* = 23.6 Hz, C-F, CH), 115.6 (d, *J* = 21.0 Hz, C-F, CH), 111.8 (CH), 108.1 (d, *J* = 26.7 Hz, C-F, CH), 61.0 ($CH_2$), 37.4 (d, *J* = 3.4 Hz, C-F, $CH_2$). Found: C, 59.60; H, 3.82; Cl, 7.96; F, 8.51; N, 12.58. Anal. calcd (%) for $C_{22}H_{17}ClF_2N_4O_2$: C, 59.67; H, 3.87; Cl, 8.00; F, 8.58; N, 12.65.

**1-(2-(2-(5-Fluoro-1-(6-chloro-2-fluorobenzyl)-2-oxoindolin-3-ylidene)hydrazinyl)-2-oxoethyl)pyridin-1-ium chloride (5b)**. Yellow powder. Yield 83%, m.p. = 152-153 °C. IR spectrum, ν, $cm^{-1}$: 1355 (C-F), 1634 (C=C), 1687 (C=O), 3017 (CH), 3393 (NH). $^1$H NMR (500 MHz, DMSO-$d_6$) δ 12.63 (s, 1H, NH), 9.10 (d, *J* = 6.1 Hz, 2H, Ar), 8.73 (t, *J* = 7.6 Hz, 1H, Ar), 8.27 (t, *J* = 6.8 Hz, 2H, Ar), 7.48-7.34 (m, 4H, Ar), 7.31-7.26 (m, 1H, Ar), 7.09-7.07 (m, 1H, Ar), 6.22 (s, 2H, $CH_2$). 5.15 (s, 2H, $CH_2$). $^{13}$C NMR (126 MHz, DMSO-$d_6$) δ 167.5, 163.5, 161.3 (d, *J* = 249.2 Hz, C-F), 158.6 (d, *J* = 239.8 Hz, C-F), 146.6 (CH), 146.5 (CH), 146.2, 139.4, 134.3 (d, *J* = 5.0 Hz, C-F, CH), 130.0 (d, *J* = 9.8 Hz, C-F, CH), 127.8 (CH), 127.7 (CH), 125.9 (d, *J* = 2.9 Hz, C-F), 120.2 (d, *J* = 16.5 Hz, C-F), 118.4 (d, *J* = 24.3 Hz, C-F, CH), 114.9 (d, *J* = 22.6 Hz, C-F, CH), 111.5 (d, *J* = 13.9 Hz, C-F), 108.1 (d, *J* = 2.3 Hz, C-F, CH), 61.1 ($CH_2$), 36.0 (d, *J* =

1.7 Hz, C-F, $CH_2$). Found: C, 55.30; H, 3.39; Cl, 14.79; F, 7.86; N, 11.70. Anal. calcd (%) for $C_{22}H_{16}Cl_2F_2N_4O_2$: C, 55.36; H, 3.38; Cl, 14.85; F, 7.96; N, 11.74.

**1-(2-(2-(5-Fluoro-2-oxo-1-(3-(trifluoromethyl)benzyl)indolin-3-ylidene)hydrazinyl)-2-oxoethyl)pyridin-1-ium chloride (5c)**. Yellow powder. Yield 79%, m.p. = 172-173 °C. IR spectrum, ν, $cm^{-1}$: 1330 (C-F), 1637 (C=C), 1702 (C=O), 1680 (C=O), 3018 (CH), 3392 (NH). $^1$H NMR (500 MHz, DMSO-$d_6$) δ 9.04 (d, *J* = 5.9 Hz, 2H, Ar), 8.71 (t, *J* = 7.8 Hz, 1H, Ar), 8.23 (t, *J* = 6.6 Hz, 2H, Ar), 7.74 (s, 1H, Ar), 7.68-7.65 (m, 2H, Ar), 7.61 (d, *J* = 7.8 Hz, 1H, Ar), 7.56-7.54 (m, 1H, Ar), 7.31-7.27 (m, 1H, Ar), 7.12 (dd, *J* = 8.8 Hz, *J* = 3.9 Hz, 1H, Ar), 6.16 (s, 2H, $CH_2$), 5.09 (s, 2H, $CH_2$). $^{13}$C NMR (126 MHz, DMSO-$d_6$) δ 168.0, 161.0, 159.2 (d, *J* = 239.8 Hz, C-F), 147.1 (CH), 146.7 (CH), 135.0, 131.8 (CH), 130.4 (CH), 129.9 (q, *J* = 31.7 Hz, C-F), 128.2 (CH), 125.0 (m, CH), 124.4 (m, CH), 124.2 (q, *J* = 272.4 Hz, C-F), 120.8, 118.8 (d, *J* = 23.7 Hz, C-F, CH), 112.2-121.1 (m, 2C, 2CH), 108.8 (d, *J* = 25.3 Hz, C-F, CH), 61.1 ($CH_2$), 42.7 ($CH_2$). $^{19}$F NMR (600 MHz, DMSO-$d_6$) δ -119.3, -61.0. Found: C, 56.00; H, 3.47; Cl, 7.17; F, 15.36; N, 11.38. Anal. calcd (%) for $C_{23}H_{17}ClF_4N_4O_2$: C, 56.05; H, 3.48; Cl, 7.19; F, 15.42; N, 11.37.

**1-(2-(2-(5-Fluoro-2-oxo-1-((perfluorophenyl)methyl)indolin-3-ylidene)hydrazinyl)-2-oxoethyl)pyridin-1-ium chloride (5d)**. Yellow powder. Yield 72%, m.p. = 165-166 °C. IR spectrum, ν, $cm^{-1}$: 1337 (C-F), 1636 (C=C), 1707 (C=O), 1731 (C=O), 3030 (CH), 3402 (NH). $^1$H NMR (600 MHz, DMSO-$d_6$) δ 12.59 (s, 1H, NH), 9.17-9.13 (m, 2H, Ar), 8.74 (t, *J* = 7.0 Hz, 1H, Ar), 8.28-8.26 (m, 2H, Ar), 7.51-7.48 (m, 1H, Ar), 7.43-7.40 (m, 1H, Ar), 7.30-7.28 (m, 1H, Ar), 6.26 (s, 2H, $CH_2$). 5.16 (s, 2H, $CH_2$). $^{13}$C NMR (151 MHz, DMSO-$d_6$) δ 167.7, 160.2, 158.7 (d, *J* = 239.8 Hz, C-F), 146.6 (CH), 146.5 (CH), 145.0 (dm, *J* = 248.2 Hz, C-F), 140.4 (dm, *J* = 252.0 Hz, C-F), 136.9 (dm, *J* = 249.4 Hz, C-F), 133.8, 127.6 (CH), 127.5 (d, *J* = 27.4 Hz, C-F, CH), 120.2, 118.5 (d, *J* = 24.0 Hz, C-F, CH), 111.6, 109.1, 107.9 (d, *J* = 26.1 Hz, C-F, CH), 61.0 ($CH_2$), 32.0 ($CH_2$). Found: C, 51.30; H, 2.50; Cl, 6.87; F, 22.08; N, 10.80. Anal. calcd (%) for $C_{22}H_{13}ClF_6N_4O_2$: C, 51.33; H, 2.55; Cl, 6.89; F, 22.14; N, 10.88.

**1-(2-(2-(5-Methyl-2-oxo-1-(3-(trifluoromethyl)benzyl)indolin-3-ylidene)hydrazinyl)-2-oxoethyl)pyridin-1-ium chloride (5e)**. Yellow powder. Yield 85%, m.p. = 202-203 °C. IR spectrum, ν, $cm^{-1}$: 1375 (C-F), 1624 (C=C), 1688 (C=O), 3011 (CH), 3402 (NH). $^1$H NMR (500 MHz, DMSO-$d_6$) δ 12.70 (s, 1H, NH), 9.14 (d, *J* = 5.7 Hz, 2H, Ar), 8.74 (t, *J* = 7.7 Hz, 1H, Ar), 8.28 (t, *J* = 7.2 Hz, 2H, Ar), 7.79 (s, 1H, Ar), 7.67-7.66 (m, 2H, Ar), 7.47 (s, 1H, Ar), 7.61 (d, *J* = 7.4 Hz, 1H, Ar), 7.47 (s, 1H, Ar), 7.28 (d, *J* = 7.3 Hz, 1H, Ar), 7.07 (d, *J* = 8.0 Hz, 1H, Ar), 6.25 (s, 2H, $CH_2$). 5.11 (s, 2H, $CH_2$), 2.33 (s, 3H, $CH_3$). $^{13}$C NMR (126 MHz, DMSO-$d_6$) δ 164.2, 163.9, 153.2, 146.6 (CH), 146.5 (CH), 140.8, 137.2, 135.2, 132.8 (CH), 132.5, 131.4, 129.8 (CH), 129.4 (q, *J* = 31.9 Hz, C-F), 127.7 (CH), 127.6 (CH), 124.4, 124.1 (CH), 124.0 (q, *J* = 273.9 Hz, C-F), 121.1, 110.4 (CH), 61.0 ($CH_2$), 42.2 ($CH_2$), 20.4 ($CH_3$). $^{19}$F NMR (600 MHz, DMSO-$d_6$) δ -61.0. Found: C, 58.90; H, 4.09; Cl, 7.27; F, 11.57; N, 11.43. Anal. calcd (%) for $C_{24}H_{20}ClF_3N_4O_2$: C, 58.96; H, 4.12; Cl, 7.25; F, 11.66; N, 11.46.

~~**1-(2-(2-(1-(2-Fluorobenzyl)-2-oxoindolin-3-ylidene)hydrazinyl)-2-oxoethyl)-2,3-dimethylpyridin-1-ium chloride (7a)**. Yellow powder. Yield 93%, m.p. = 180-181 °C with decomposition. IR spectrum, ν, $cm^{-1}$: 1353 (C-F), 1614 (C=C), 1689 (C=O), 1720 (C=O), 3017 (CH), 3399 (NH). $^1$H NMR (600 MHz, $CDCl_3$) δ 12.78 (s, 1H, NH), 9.55 (d, *J* = 5.8 Hz, 1H, Ar), 8.22 (d, *J* = 7.8 Hz, 1H, Ar), 7.89 (d, *J* = 7.5 Hz, 1H, Ar), 7.80 (t, *J* = 6.7 Hz, 1H, Ar), 7.29-7.23 (m, 3H, Ar), 7.09-7.04 (m, 3H, Ar), 6.77 (d, *J* = 7.9 Hz, 1H, Ar), 6.72 (s, 2H, $CH_2$), 4.88 (s, 2H, $CH_2$), 2.75 (s, 3H, $CH_3$), 2.54 (s, 3H, $CH_3$). $^{13}$C NMR (151 MHz, $CDCl_3$) δ 166.5, 160.9, 160.5 (d, *J* = 246.8 Hz, C-F), 155.2, 146.5 (CH), 146.1 (CH), 142.7, 138.2, 135.9, 132.1 (CH), 130.0 (d, *J* = 8.1 Hz, C-F, CH), 129.7 (d, *J* = 3.1 Hz, C-F, CH), 124.9 (CH), 124.5 (d, *J* = 3.3 Hz, C-F, CH), 123.9 (CH), 122.8 (CH), 121.6 (d, *J* = 14.4 Hz, C-F), 118.9, 115.6 (d, *J* = 24.4 Hz, C-F, CH), 109.5 (d, *J* = 1.7 Hz, C-F, CH), 60.4 ($CH_2$), 36.9 (d, *J* = 4.7 Hz, C-F, $CH_3$), 20.2 ($CH_3$), 17.7 ($CH_3$). Found: C, 57.90; H, 4.41; Br, 16.00; F, 3.76; N, 11.23. Anal. calcd (%) for $C_{24}H_{23}BrFN_4O_2$: C, 57.96; H, 4.46; Br, 16.07; F, 3.82; N, 11.26.~~

~~**1-(2-(2-(1-(2-Chloro-6-fluorobenzyl)-2-oxoindolin-3-ylidene)hydrazinyl)-2-oxoethyl)-2,3-dimethylpyridin-1-ium chloride (7b)**. Yellow powder. Yield 94%, m.p. = 197-198 °C. IR spectrum, ν, $cm^{-1}$: 1352 (C-F), 1614 (C=C), 1691 (C=O), 1716 (C=O), 3018 (CH), 3400 (NH). $^1$H NMR (600 MHz, $CDCl_3$/DMSO-$d_6$) δ 12.77 (s, 1H, NH), 9.05 (d, *J* = 4.5 Hz,~~

~~1H, Ar), 8.39 (d, *J* = 7.7 Hz, 1H, Ar), 7.85 (t, *J* = 6.9 Hz, 1H, Ar), 7.66 (d, *J* = 6.5 Hz, 1H, Ar), 7.34 7.30 (m, 2H, Ar), 7.24 (d, *J* = 8.0 Hz, 1H, Ar), 7.11 7.05 (m, 2H, Ar), 6.88 (d, *J* = 8.0 Hz, 1H, Ar), 6.31 (s, 2H, $CH_2$). 5.09 (s, 2H, $CH_2$), 2.69 (s, 3H, $CH_3$), 2.55 (s, 3H, $CH_3$). $^{13}$C NMR (151 MHz, $CDCl_3$/DMSO *d*$_6$) δ 166.1, 160.9, (d, *J* = 250.6 Hz, C-F), 159.9, 155.3, 146.4 (CH), 144.7 (CH), 142.5, 138.0, 134.7, 134.4 (CH), 131.8 (CH), 130.3 (d, *J* = 9.3 Hz, C-F, CH), 125.5 (CH), 124.3 (CH), 123.0 (CH), 120.8 (CH), 119.5 (d, *J* = 15.7 Hz, C-F), 118.4, 114.3 (d, *J* = 22.5 Hz, C-F, CH), 109.6 (CH), 59.1 ($CH_2$), 36.2 ($CH_2$), 19.4 ($CH_3$), 16.7 ($CH_3$). Found: C, 54.16; H, 3.96; Br, 14.97; Cl, 6.60; F, 3.49; N, 10.51. Anal. calcd (%) for $C_{24}H_{21}BrClFN_5O_2$: C, 54.20; H, 3.98; Br, 15.02; Cl, 6.67; F, 3.57; N, 10.54.~~

~~**1-(2-(2-(1-(3-Trifluoromethylbenzyl)-2-oxoindolin-3-ylidene)hydrazinyl)-2-oxoethyl)-2,3-dimethylpyridin-1-ium chloride (7e)**. Yellow powder. Yield 90%, m.p. = 176-177 °C. IR spectrum, ν, cm$^{-1}$: 1360 (C-F), 1617 (C=C), 1691 (C=O), 1719 (C=O), 3018 (CH), 3413 (NH). $^1$H NMR (400 MHz, $CDCl_3$/DMSO *d*$_6$) δ 12.78 (s, 1H, NH), 9.18 (d, *J* = 5.2 Hz, 1H, Ar), 8.34 (d, *J* = 7.8 Hz, 1H, Ar), 7.81 (t, *J* = 6.8 Hz, 1H, Ar), 7.71 (d, *J* = 7.1 Hz, 1H, Ar), 7.56 (s, 1H, Ar), 7.53 7.50 (m, 2H, Ar), 7.47 (d, *J* = 7.6 Hz, 1H, Ar), 7.33 (dd, *J* = 7.7 Hz, *J* = 7.6 Hz, 1H, Ar), 7.10 (dd, *J* = 7.1 Hz, *J* = 7.1 Hz, 1H, Ar), 6.89 (d, *J* = 7.9 Hz, 1H, Ar), 6.40 (s, 2H, $CH_2$). 5.01 (s, 2H, $CH_2$), 2.70 (s, 3H, $CH_3$), 2.55 (s, 3H, $CH_3$). $^{13}$C NMR (101 MHz, $CDCl_3$/DMSO *d*$_6$) δ 165.9, 160.4, 155.1, 146.3 (CH), 144.9 (CH), 142.4, 138.0, 135.7, 135.0, 131.8 (CH), 130.5 (CH), 130.3 (q, *J* = 32.1 Hz, C-F), 129.1 (CH), 124.3 (CH), 123.6 (2CH, overlapped), 123.3 (CH), 121.3 (CH), 118.4, 109.7 (CH), 59.2 ($CH_2$), 42.4 ($CH_2$), 19.5 ($CH_3$), 16.8 ($CH_3$). The signal of carbon atom of $CF_3$-group is not observed. Found: C, 54.83; H, 4.00; Br, 14.58; F, 10.37; N, 10.20. Anal. calcd (%) for $C_{25}H_{22}BrF_3N_4O_2$: C, 54.86; H, 4.05; Br, 14.60; F, 10.41; N, 10.24.~~

Formatted: MDPI_3.1_text

### *3.2 Biological Studies*

**Anticancer activity**

**Cell lines and their cultivation**

Human cell cultures of tumor origin - HeLa (cervical tumor), HuTu 80 (human duodenal adenocarcinoma) - and normal cell line ChangLiver (human normal hepatocyte)), provided by the Laboratory of Tumor Cell Genetics of the Scientific Research Institute of Carcinogenesis, N.N. Blokhin National Medical Research Center of Oncology, as well as the Institute of Cytology of the Russian Academy of Sciences, were grown in a nutrient medium DMEM (PanEco, Moscow, Russia) and MEM (PanEco, Moscow, Russia), containing fetal bovine serum (10% by volume) (ThermoFisher Scientific, Paisley, UK), Glutamax (2 mM) (Gibco, Scotland, UK), and penicillin-streptomycin (1% by volume) (PanEco, Moscow, Russia). The cultivation was carried out at 37°C in a humidified $CO_2$ atmosphere (5%).

**Determination of Cell Viability**

Cell viability was determined by MTT test [~~50~~81]. Cells were seeded in a 96-well plate in the amount of $1*10^4$ cells/200 µl of complete nutrient medium and cultured at 37°C in $CO_2$ (5%). After 24 hours of incubation, various concentrations of test compounds in the range from 0.1 to 100 µM, were added to the cell cultures, and then the cells were cultured under the same conditions for 24 and 72 hours. For each concentration, the experiment was carried out in triplicate.

All compounds were dissolved in DMSO, then diluted with the medium to the required concentration. The final content of DMSO in the well did not exceed 1% and did not have a toxic effect on the cells. The DMSO also was added to the control wells in a volume of 1%. After the incubation time, MTT (3-(4,5-dimethylthiazol-2-yl)-2,5-diphenyltetrazolium bromide, 5 mg/ml) was added to each well and plates were additionally incubated for 2 hours (until the characteristic color appeared).

Using a plate analyzer (Cytation3, BioTech Instruments Inc., USA), the optical density was determined at 530 nm. The concentration value causing 50% inhibition of cell population growth ($IC_{50}$) was determined from dose-dependent curves.

The $IC_{50}$ parameter was calculated using the AAT Bioquest program [82].

The selectivity index (SI) is calculated as the ratio between the $IC_{50}$ for normal cells and the $IC_{50}$ for cancer cells [83].

**Apoptosis**

HuTu 80 cells at 1 × $10^6$ cells/well in a final volume of 2 ml were seeded into six-well plates. After 24 h of incubation, various concentrations of tested compounds were added to wells. The cells were harvested at 2000 rpm for 5 min and, then, washed twice with ice-cold PBS, followed by resuspension in binding buffer. Next, the samples were incubated with 5 µl of annexin V- Alexa Fluor 647 (Sigma-Aldrich, USA) and 5 µl of propidium iodide for 15 min at room temperature in the dark. Finally, the cells were analyzed by flow cytometry (Guava easy Cyte, MERCK, USA) within 1 h. The experiments were repeated three times.

**ROS**

HuTu 80 cells were incubated with tested compounds at concentrations of $IC_{50}$ for 24 hours. ROS generation was investigated using flow cytometry assay and CellROX® Deep Red flow cytometry kit. For this HuTu 80 cells were harvested at 2000 rpm for 5 minutes and then washed twice with ice-cold PBS, followed by resuspension in 0.1 ml of medium without FBS, to which was added 0.2 µL of CellROX® Deep Red and incubated at 37 ° C for 30 minutes After three times washing the cells and suspending them in PBS, the production of ROS in the cells was immediately monitored using flow cytometer Guava easy Cyte, MERCK, USA).

**Anticoagulant and Anti-aggregation Activities Study**

The in vitro experiments were performed using the blood of healthy male donors aged 18-24 years (total 54 donors). The study was approved by the Ethics Committee of Federal State Budgetary Educational Institution of Higher Education at the Bashkir State Medical University of the Ministry of Health of Russian Federation (No.2 dated 17.10.2012). Informed consent was obtained from all participants before blood sampling. The blood was collected from the cubital vein using the system of vacuum blood collection BD Vacutainer® (Becton, Dickinson and Company, USA). A 3.8 % sodium citrate solution in a 9:1 ratio was used as a venous blood stabiliser. The study of the effect on platelet aggregation was performed using the Born method [~~83~~84] using the aggregometer «AT-02» (SPC Medtech, Russia). The assessment of antiplatelet activity of the studied compounds and reference preparations was started with the final concentration of 2×10–3 mol/L. Adenosine diphosphate (ADP; 20 µg/mL) and collagen (5 mg/mL) manufactured by Tehnologia-Standart Company, Russia, were used as inducers of aggregation. The study on the anticoagulant activity was performed by standard recognised clotting tests using the optical two-channel automatic analyser of blood coagulation Solar CGL 2110 (CJSC SOLAR, Belarus). The following parameters were studied: activated partial thromboplastin time (APTT), prothrombin time (PT) and fibrinogen concentrations according to the Clauss method. The determination of anticoagulant activity of the studied compounds and reference preparation was performed in a concentration of 5×10–4 g/mL using the reagents manufactured by Tehnologia-Standart Company (Barnaul, Russia). The results of the study were processed using the statistical package Statistica 10.0 (StatSoft Inc, USA). The Shapiro–Wilk's test was used to check the normality of actual data distribution. The form of distribution of the data obtained differed from the normal one; therefore, non-parametric methods were used for further analysis. The data were presented as medians and 25 and 75 percentiles. Analysis of variance was conducted using Kruskal–Wallis test. A p value of 0.05 was considered statistically significant.

**Antiphytopathogenic activity**

Plant pathogenic bacterial strains *Micrococcus luteus* B-109, *Pectobacterium atrosepticum* 1043, *Pectobacterium carotovorum* subsp. *carotovorum* MI, *Pseudomonas fluorescens* EL-2.1, and *Xanthomonas campestris* B-610 and fungal strain *Fusarium oxysporum* IBPPM 543 were from the Collection of Rhizosphere Microorganisms, IBPPM RAS (WFCC no. 975, WDCM no. 1021) (CM IBPPM, http://collection.ibppm.ru). Pathogenic fungus *Phytophthora cactorum* VKM F-985 provided by the All-Russian Collection of Microorganisms (VKM) and deposited at A.E. Favorsky Irkutsk Institute of Chemistry, SB RAS, was also used as test

organism. Bacteria *M. luteus*, *P. carotovorum* subsp. *carotovorum*, *P. atrosepticum*, and *Ps. fluorescens* were grown in meat-peptone medium (BP), and *X. campestris* was grown in the medium with glucose, yeast extract, and calcium carbonate (GYCa). Solid media contained Bacto agar (18 g/L); pH was adjusted to 7.2-7.4. All bacterial cultures were grown at 28°C. The mycelial cultures of *F. oxysporum* and *P. cactorum* were grown on a glucose-peptone-yeast (GPY) nutrient medium at 27°C. For inoculum preparation, both fungal strains were initially grown on the agar GPY in Petri dishes, and then transferred into the seed medium by punching out 5 mm of the agar plate culture with a self-designed cutter.

Antibacterial and antifungal activities of the compounds were explored using the agar well diffusion method and the technique of a mycelial radial growth inhibition. Method of diffusion in agar (measuring the diameter of growth inhibition zones) was used for determining the bactericidal activity. The 6-mm wells were made in agar medium (GYCa for *Xanthomonas campestris* or BP for other bacteria). Bacterial suspensions were distributed over the agar surface, and the tested compound's solution (150 μl) was added to each well. The width of growth inhibition zones around the wells was determined after incubation for 36-40 h.

For the fungicidal activity analysis, radial growth (colony diameters) of the fungi on a solid medium in the absence and in the presence of the compounds **5a-e, 7a-c** solutions at various concentrations were compared. The method consisted in the following: sterile, melted and then cooled to about 60°C GPY agar medium (20.0 ml) was mixed with the precisely measured volumes of the solutions under question, and poured into a sterile Petri dish (90 mm i.d.). After solidification of GPY agar, the media were inoculated by the fungus using 10-day-old cultures of *F. oxysporum* or *P. cactorum*. The inoculation was done by transferring a 5-mm (i.d.) GPY-agar block covered with mycelium to the center of the Petri dish followed by incubation in a thermostat at 27°C. The fungicidal effect was scored by the size of mycelium colony on a Petri dish compared to the control without fungicidal admixtures to GPY agar. Each treatment was performed in at least four replicates in two independent experiments. The observation period ended when the control Petri dish was filled with mycelium (usually after 12 days). The inhibition of the phytopathogen colony growth by the compounds **5a-e, 7a-c** or the reference fungicides solutions was calculated as a percentage by which the mycelium radial propagation was decreased compared to the unaffected control, the latter was taken as 100% of growth (or zero percent of inhibition). The $EC_{50}$ value was calculated as the compound concentration at which the radial growth of the fungus colony was decreased by 50% relative to the non-fungicidal control. This effective concentration causing 50% of the fungal growth inhibition was determined from the dose-relative inhibition curves plotted for each tested compound, according with the approach developed *e.g.* in Refs [78, 79]. The solutions of compounds **5a-e, 7a-c** were prepared with a concentration of 2 mmol/l (stock solution). For comparison, test compounds were also a commonly applied disinfecting agents and antibiotics used as a positive control.

**Statistical Analysis**

The data was expressed as mean ± SEM. Statistical comparisons were made using one-way analysis of variance (ANOVA) followed by Dunnett's Multiple Comparison tests. Two-way repeated measures (mixed model) ANOVA followed by Bonferroni post-tests were also used to compare the recognition of two objects. A difference with p value ≤ 0.05 was considered statistically significant. The statistical analysis was performed using GraphPad Prism 5 (GraphPad Software, San Diego, CA, USA).

## 5. Conclusions

A series of novel fluorinated 1-benzylisatins was synthesized with high yields by easy one-pot reaction procedure. Using the acid-catalyzed reaction of new isatins with Girard's reagent P and its dimethyl analogue, a wide range of water-soluble isatin-3-hydrazones was obtained. The most promising use of modified isatins as a basis for the creation of anticancer agents is possessed by ortho-substituted fluorine (**3a**), chlorine (**3b**), or both (**3d**) atoms in the benzyl fragment of the com-

pound. The mechanism of the cytotoxic action of these substances is associated with apoptosis induction due to mitochondrial membrane dissipation and stimulation of reactive oxygen species production in tumor cells. It was shown that compounds **3a** and **3b** exhibit antiaggregation activity at the level of acetylsalicylic acid, and the whole series of fluorine-containing isatins does not adversely affect the hemostasis system as a whole. In a wide range of new water-soluble pyridinium isatin-3-acylhydrazones, substances **7c** and **5c,e** exhibit the highest activity. They have an antagonistic effect against phytopathogens of bacterial and fungal origin and can be considered as biological preparations for combating plant diseases.

**Supplementary Materials:** The following supporting information can be downloaded at: www.mdpi.com/xxx/s1, Table S1, Figures S1–S2 – X-Ray crystallography data, Tables S2-S5 - antiphytopathogenic activity data, Figures S6–S56 - copies of NMR spectra of all synthesized compounds.

**Author Contributions:** A.B. — investigation (chemistry), writing—original draft preparation, supervision (chemistry), I.L. — investigation (X-ray study), N.Ak. — investigation (chemistry), A.V., A.L., S.G., O.M., Z.V., A.S., M.N. — investigation (*in vitro* study), R.Zh. — funding acquisition, I.A. — project administration. All authors have read and agreed to the published version of the manuscript.

**Funding:** The synthesis, the studies of anticancer and antimicrobial activities were carried out at Arbuzov Institute of Organic and Physical Chemistry and was supported by the Ministry of Science and Higher Education of the Russian Federation at FRC Kazan Scientific Center (grant No. 075-15-2022-1128). The study of hemolytic activity was funded by the Non-Profit Joint-Stock Company "Korkyt Ata Kyzylorda University". Evaluation of antiphytopathogenic activity was completed in the framework of theme No. 121031100266-3 of the Program of fundamental research of the Russian Academy of Sciences.

**Informed Consent Statement:** Not applicable

**Acknowledgments:** The authors are grateful to the Assigned Spectral-Analytical Center of FRC Kazan Scientific Center of RAS for technical assistance in research.

**Conflicts of Interest:** The authors declare no conflicts of interest.

**Sample Availability:** Samples of all described compounds are available from the author A. Bogdanov.

## References

1. Zhang, Sh.; Huang, D.; Wu, J.; Wang, Z. Decade Advance of Isatin in Three-component Reactions. *Asian J. Org. Chem.* **2023**, *12*, e202200591, doi:10.2174/1389557511313080001.
2. Pradeep, S.D., Mohanan, P.V. Advancements in Schiff Bases of 1H-Indole-2,3-dione: A Versatile Heterocyclic Compound in Pharmacological Field. *Mini-Rev. Org. Chem.* **2023**, *20*, 45–54, doi:10.2174/1570193X19666220309142035.
3. Efremov, A.M.; Beznos, O.V.; Eremeev, R.O.; Chesnokova, N.B.; Milaeva, E.R.; Shevtsova, E.F.; Lozinskaya, N.A. Microwave-Assisted Synthesis of 3-Hydroxy-2-oxindoles and Pilot Evaluation of Their Antiglaucomic Activity. *Int. J. Mol. Sci.* **2023**, *24*, 5101, doi:10.3390/ijms24065101.
4. Nath, R.; Pathania, Sh.; Grover, G.; Akhtar, M. Isatin containing heterocycles for different biological activities: Analysis of structure activity relationship. *J. Mol. Struct.* **2020**, *1222*, 128900, doi:10.1016/j.molstruc.2020.128900.
5. Gupta, A.K.; Tulsyan, S.; Bharadwaj, M.; Mehrotra, R. Systematic Review on Cytotoxic and Anticancer Potential of *N*-Substituted Isatins as Novel Class of Compounds Useful in Multidrug-Resistant Cancer Therapy: In Silico and In Vitro Analysis. *Top. Curr. Chem.* **2019**, *377*, 15, doi:10.1007/s41061-019-0240-9.
6. Mushtaq, A.; Azam, U.; Mehreen, S.; Naseer, M.M. Synthetic α-glucosidase inhibitors as promising anti-diabetic agents: Recent developments and future challenges. *Eur. J. Med. Chem.* **2023**, *249*, 115119, doi:10.1016/j.ejmech.2023.115119.
7. Cheke, R.S., Firke, S.D., Patila, R.R., Bari, S.B. Isatin: new hope against convulsion. *Central Nervous System Agents Med. Chem.* **2018**, *18*, 76–101, doi:10.2174/1871524917666171113124112.
8. Saini, T., Kumar, S., Narasimhan, B. Central nervous system activities of Indole derivatives: an overview. *Central Nervous System Agents Med. Chem.* **2015**, *16*, 19–28, doi:10.2174/1871524915666150608103224.
9. Medvedev, A., Igosheva, N., Crumeyrolle-Arias, M., Glover, V. Isatin: role in stress and anxiety. *Stress* **2005**, *8*, 175–183, doi:10.1080/10253890500342321.
10. Zhang, M. Z., Chen, Q., Yang, G. F. A review on recent developments of indole-containing antiviral agents. *Eur. J. Med. Chem.* **2015**, *89*, 421–441, doi:10.1016/j.ejmech.2014.10.065.

Formatted: Font: Bold
Formatted: Font: Bold
Formatted: Russian

11. Bharathi Dileepan, A. G., Daniel Prakash, T., Ganesh Kumar, A., Shameela Rajam, P., Violet Dhayabaran, V., Rajaram, R. Isatin based macrocyclic Schiff base ligands as novel candidates for antimicrobial and antioxidant drug design: in vitro DNA binding and biological studies. *J. Photochem. Photobiol. B Biol*. **2018**, *183*, 191–200. doi:10.1016/j.jphotobiol.2018.04.029.
12. Xu, Z., Zhang, S., Gao, C., Fan, J., Zhao, F., Lv, Z. S., Feng, L. S. Isatin hybrids and their anti-tuberculosis activity. *Chinese Chem. Lett*. **2017**, *28*, 159–167. doi:10.1016/j.cclet.2016.07.032.
13. Raj, R., Gut, J., Rosenthal, P. J., Kumar, V. 1H-1,2,3-triazole-tethered isatin-7-chloroquinoline and 3-hydroxy-indole-7-chloroquinoline conjugates: synthesis and antimalarial evaluation. *Bioorg. Med. Chem. Lett.* **2014**, *24*, 756–759, doi:10.1016/j.bmcl.2013.12.109.
14. Rodríguez-Argüelles, M. C., Cao, R., García-Deibe, A. M., Pelizzi, C., Sanmartín-Matalobos, J., Zani, F. Antibacterial and antifungal activity of metal(II) complexes of acylhydrazones of 3-isatin and 3-(N-methyl)isatin. *Polyhedron* **2009**, *28*, 2187–2195, doi:10.1016/j.poly.2008.12.038.
15. Guo, H. Isatin derivatives and their anti-bacterial activities. *Eur. J. Med. Chem*. **2019**, *164*, 678–688, doi:10.1016/j.ejmech.2018.12.017.
16. Ferraz de Paiva, R.E.; Vieira, E.G.; Rodrigues da Silva, D.; Wegermann, C.A.; Costa Ferreira, A.M. Anticancer Compounds Based on Isatin-Derivatives: Strategies to Ameliorate Selectivity and Efficiency. *Front. Mol. Biosci.* **2021**, *7*, 627272, doi:10.3389/fmolb.2020.627272.
17. Rizzo, M., Porta, C. Sunitinib in the treatment of renal cell carcinoma: An update on recent evidence. *Ther. Adv. Urol*. **2017**, *9*, 195–207, doi:10.1177/1756287217713902
18. Nadagouda, M.; Vijayasarathy, P.; Sin, A.; Nam, H.; Khan, S.; Parambath, J.B.M.; Mohamed, A.; Han, Ch. Antimicrobial activity of quaternary ammonium salts: structure-activity relationship. *Med. Chem. Res.* **2022**, *31*, 1663–1678, doi:10.1007/s00044-022-02924-9.
19. Dan, W.; Gao, J.; Qi, X.; Wang, J.; Dai, J. Antibacterial quaternary ammonium agents: Chemical diversity and biological mechanism. *Eur. J. Med. Chem.* **2022**, *243*, 114765, doi:10.1016/j.ejmech.2022.114765.
20. Morrison, K.R.; Allen, R.A.; Minbiole, K.P.C.; Wuest, W.M. More QACs, more questions: Recent advances in structure activity relationships and hurdles in understanding resistance mechanisms. *Tetrahedron Lett.* **2019**, *60*, 150935, doi:10.1016/j.tetlet.2019.07.026.
21. Vereshchagin, A.N.; Frolov, N.A.; Egorova, K.S.; Seitkalieva, M.M.; Ananikov, V.P. Quaternary Ammonium Compounds (QACs) and Ionic Liquids (ILs) as Biocides: From Simple Antiseptics to Tunable Antimicrobials. *Int. J. Mol. Sci.* **2021**, *22*, 6793, doi:10.3390/ijms22136793.
22. Sharma, V.D.; Aifuwa, E.O.; Heiney, P.A.; Ilies, M.A. Interfacial engineering of pyridinium gemini surfactants for the generation of synthetic transfection systems. *Biomaterials* **2013**, *34*, 6906–6921, doi:10.1016/j.biomaterials.2013.05.029.
23. Pashirova, T.N.; Shaihutdinova, Z.M.; Vandyukov, A.E.; Voloshina, A.D.; Samorodov, A.V.; Pavlov, V.N.; Souto, E.B.; Mironov, V.F.; Bogdanov, A.V. Synthesis and structure-activity-toxicity relationships of DABCO containing ammonium amphiphiles based on natural isatin scaffold. *J. Mol. Liq.* **2022**, *365*, 120217, doi:10.1016/j.molliq.2022.120217.
24. Chugunova, E.; Samsonov, V.; Gerasimova, T.; Rybalova, T.; Bagryanskaya, I. Synthesis and some properties of 2H-benzimidazole 1,3-dioxides. *Tetrahedron* **2015**, *71*, 7233-7244, doi:10.1016/j.tet.2015.03.096.
25. Bogdanov, A.; Tsivileva, O.; Voloshina, A.; Lyubina, A.; Amerhanova, S.; Burtceva, E.; Bukharov, S.; Samorodov, A.; Pavlov, V. Synthesis and diverse biological activity profile of triethyl-ammonium isatin-3-hydrazones. *ADMET & DMPK* **2022**, *10*, 163-179. doi:10.5599/admet.1179.
26. Bogdanov, A.V.; Zaripova, I.F.; Voloshina, A.D.; Sapunova, A.S.; Kulik, N.V.; Tsivunina, I.V., Dobrynin, A.B.; Mironov, V.F. Isatin derivatives bearing a fluorine atom. Part 1: Synthesis, hemotoxicity and antimicrobial activity evaluation of fluorobenzylated water-soluble pyridinium isatin-3-acylhydrazones. *J. Fluorine Chem.* **2019**, *227*, 109345, doi:10.1016/j.jfluchem.2019.109345.
27. Chugunova, E.A.; Akylbekov, N.I.; Appazov, N.O.; Makhrus, E.M.; Burilov, A.R. Synthesis of the First Tertiary Ammonium Derivative of 6-Chloro-5-nitrobenzofuroxan. *Russ. J. Org. Chem.* **2016**, *52*, 920-921, doi:10.1134/S1070428016060312.
28. Zhou, Y.; Wang, J.; Gu, Zh.; Wang, Sh.; Zhu, W.; Acena, J.L.; Soloshonok, V.A.; Izawa, K.; Liu, H. Next generation of fluorine-containing pharmaceuticals, compounds currently in phase II–III clinical trials of major pharmaceutical companies: new structural trends and therapeutic areas. *Chem. Rev.* **2016**, *116*, 422-518, doi:10.1021/acs.chemrev.5b00392.
29. Gillis, E.; Eastman, K.J.; Hill, M.D.; Donnelly, D.J.; Meanwell, N.A. Applications of fluorine in medicinal chemistry. *J. Med. Chem.* **2015**, *58*, 8315-8359, doi:10.1021/acs.jmedchem.5b00258.
30. Alabugin I.V.; Manoharan, M.; Peabody S.; Weinhold, F. The Electronic Basis of Improper Hydrogen Bonding: A Subtle Balance of Hyperconjugation and Rehybridization. *J. Am. Chem. Soc.* **2003**, *125,* 5973-5987, doi: 10.1021/ja034656e.
31. Pandey, V.K.; Dwivedi, A.; Pandey, O.P..; Sengupta, S.K. *J. Agric Food Chem.* **2008**, *56*, 10779, doi:10.1021/jf801975z.
32. Zampirolli, L.S.; de Lemos, M.J;. Goncalves, V.T.; de Souza, M.A.A.; de Souza, S.R.; Rumjanek, V.M.; DaCosta, J.B.N. *Quim. Nova* **2014**, *37*, 989, doi:10.1016/j.dib.2018.08.073.
33. Smolobochkin, A.V.; Gazizov, A.S.; Yakhshilikova, L.J.; Bekrenev, D.D.; Burilov, A.R.; Pudovik, M.A.; Lyubina, A.P.; Amerhanova, S. K.; Voloshina, A.D. Synthesis and Biological Evaluation of Taurine-Derived Diarylmethane and Dibenzoxanthene Derivatives as Possible Cytotoxic and Antimicrobial Agents. *Chem. Biodiversity* **2022**, *19*, e202100970, doi:10.1002/cbdv.202100970.
~~34. AAT Bioquest, Inc. (2022, March 17). Quest Graph™ IC50 Calculator. AAT Bioquest.~~
~~35.~~3

~~34. Ayoup, M.; Wahby,Y.; Abdel-Hamid, H.; Ramadan, E.; Teleb, M.; Abu-Serie, M.; Noby, A. Design, synthesis and biological evaluation of novel 2-acyloxy carboxamides via Passerini reaction as caspase 3/7 activators. *Eur. J. Med. Chem.* **2019**, *168*, 340-356, doi:10.1016/j.ejmech.2019.02.051.~~

~~36~~. Meier, P.; Finch, A.; Evan, G. Apoptosis in development. *Nature* **2000**, *407*, 796–801, doi:10.1038/35037734.

~~37~~35. Andreeva, O.V.; Sapunova, A.S.; Lyubina, A.P.; Amerhanova, S.K.; Belenok, M.G.; Saifina, L.F.; Semenov, V.E.; Kataev, V.E. Synthesis, antimicrobial activity and cytotoxicity of triphenylphosphonium (TPP) conjugates of 1,2,3-triazolyl nucleoside analogues. *Bioorg. Chem.* **2021**, *116*, 105328, doi:10.1016/j.bioorg.2021.105328.

~~38~~36. Mironov, V.F.; Nemtarev, A.V.; Tsepaeva, O.V.; Dimukhametov, M.N.; Litvinov, I.A.; Voloshina, A.D.; Pashirova, T.N.; Titov, E.A.; Lyubina, A.P.; Amerhanova, S.K.; Gubaidullin, A.T.; Islamov, D.R. Rational design 2-hydroxypropylphosphonium salts as cancer cell mitochondria-targeted vectors: synthesis, structure, and biological properties. *Molecules* **2021**, *26*, 6350, doi: 10.3390/molecules26216350.

~~39~~37. Haemmerle, M.; Stone, R.L.; Menter, D.G.; Afshar-Kharghan, V.; Sood, A.K. The Platelet Lifeline to Cancer: Challenges and Opportunities. *Cancer Cell* **2018**, *33*, 965-983, doi:10.1016/j.ccell.2018.03.002.

~~40~~38. Morris, K.; Schnoor, B.; Papa, A.L. Platelet cancer cell interplay as a new therapeutic target. *Biochim. Biophys. Acta. Rev. Cancer*. **2022**, *1877(5)*, 188770, doi:10.1016/j.bbcan.2022.188770.

~~41~~39. Suzuki-Inoue, K. Platelets and cancer-associated thrombosis: focusing on the platelet activation receptor CLEC-2 and podoplanin. *Blood* **2019**, *134*, 1912-1918, doi:10.1182/blood.2019001388.

~~42~~40. Tao, D.L..; Tassi Yunga, S..; Williams, C.D..; McCarty, O.J.T. Aspirin and antiplatelet treatments in cancer. *Blood* **2021**, *137*, 3201–3211, doi:10.1182/blood.2019003977.

~~43~~41. Ma, Y.; Li, G.; Yu, M.; Sun, X.; Nian, J.; Gao, Y.; Li, X.; Ding, T.; Wang, X. Prognostic significance of thrombocytosis in lung cancer: a systematic review and meta-analysis. *Platelets* **2021**, *32*, 919-927, doi:10.1080/09537104.2020.1810653.

~~44~~42. Ishizuka, M.; Nagata, H.; Takagi, K.; Iwasaki, Y.; Kubota, K. Preoperative thrombocytosis is associated with survival after surgery for colorectal cancer. *J. Surg. Oncol*. **2012**, *106*, 887-891, doi:10.1002/jso.23163

~~45~~43. He, Y.; Xia, T.; Bian, H.; Zhuo, Z.; Lu, H.; Wang, Z. Pretreatment thrombocytosis predicts survival in colorectal cancer. *Clin. Res. Hepatol. Gastroenterol.* **2016**, *40*, e59-e60, doi:10.1016/j.clinre.2016.04.002.

~~46~~44. Gu, D.; Szallasi, A. Thrombocytosis Portends Adverse Prognosis in Colorectal Cancer: A Meta-Analysis of 5,619 Patients in 16 Individual Studies. *Anticancer Res.* **2017**, *37*, 4717-4726, doi:10.21873/anticanres.11878.

~~47~~45. Mezei, T.; Bode, I.; Tenke, P.; Josa, V.; Merkel, K.; Szilasi, Z.; Tordai, A.; Mathe, D.; Baranyai, Z. The Correlation Between Platelet Count and Survival in Prostate Cancer. *Res. Rep. Urol*. **2022**, *14*, 193-202, doi:10.2147/RRU.S359715.

~~48~~46. Sylman, J.L.; Boyce, H.B.; Mitrugno, A.; Tormoen, G.W.; Thomas, I.C.; Wagner, T.H.; Lee, J.S.; Leppert, J.T.; McCarty, O.J.T.; Mallick, P. A Temporal Examination of Platelet Counts as a Predictor of Prognosis in Lung, Prostate, and Colon Cancer Patients. *Sci Rep*. **2018**, *8*, 6564. doi:10.1038/s41598-018-25019-1.

~~49~~47. Hufnagel, D.H.; Cozzi, G.D.; Crispens, M.A.; Beeghly-Fadiel, A. Platelets, Thrombocytosis, and Ovarian Cancer Prognosis: Surveying the Landscape of the Literature. *Int. J. Mol. Sci*. **2020**, *21*, 8169, doi:10.3390/ijms21218169.

~~50~~48. Xu, X.R.; Yousef, G.M.; Ni, H. Cancer and platelet crosstalk: opportunities and challenges for aspirin and other antiplatelet agents. *Blood* **2018**, *131*, 1777-1789, doi:10.1182/blood-2017-05-743187.

~~51~~49. Downer, M.; Allard, C.; Preston, M.; Gaziano, J.M.; Stampfer, M.J.; Mucci, L.A.; Batista, J.L. Regular aspirin use and the risk of lethal prostate cancer in the Physicians Health Study. *Eur. Urol*. **2017**, *72*, 821-827, doi:10.1016/j.eururo.2017.01.044.

~~52~~50. Chen, W.Y.; Ballman, K.V.; Winer, E.P.; Openshaw, Th.H.; Hahn, O.M.; Briccetti, F.M.; Johnson Irvin, W.; Pohlmann, P.R.; Carey, L.A.; Partridge, A.H.; Weiss, A.; McCall, L.M.; Matyka, C.; Carvan, M.; Holmes, M.D. A randomised Phase III double-blinded placebo-controlled trial of aspirin as adjuvant therapy for breast cancer (A011502). *J. Clin. Oncol*. **2022**, *40*, 360922, doi:10.1200/JCO.2022.40.36.

~~53~~51. Jafa, E.; L, Ch.; Nisha, Y.; Kate, V.; Kayal, S.; Ganesh, R.N.; Sunitha, V.C.; Ganesan, P.; Penumadu, P.; Dubashi, B. Comparison of efficacy of aspirin plus EOX vs. EOX alone in patients with locally advanced and metastatic gastric cancer: a randomised clinical trial. *J. Gastrointest. Cancer* **2022**, Jul 16, doi:10.1007/s12029-022-00845-9.

~~54~~52. Jothi Nayaki, S.; Ramya, R.; Srividhya, S.; Kiruthika, J.; Ramya, K.; Karthiga, S.; Arunachalam, M.; Kavitha, D. Antibacterial potentials of pillar[5]arene, pillar[4]arene[1]quinone derivative and their isatin inclusion complexes. *Supramol. Chem*. **2021**, *33*, 701-708, doi:10.1080/10610278.2023.2173072.

~~55~~53. Abd-El-Khair, H.; Abdel-Gaied, T.G.; Mikhail, M.S.; Abdel-Alim, A.I.; El-Nasr, H.I.S. Biological control of Pectobacterium carotovorum subsp. carotovorum, the causal agent of bacterial soft rot in vegetables, in vitro and in vivo tests. *Bull. Natl. Res. Cent*. **2021**, *45*, 37, doi:10.1186/s42269-021-00491-4.

~~56~~54. Huang, X.; Ren, J.; Li, P.; Feng, S.; Dong, P.; Ren, M. Potential of microbial endophytes to enhance the resistance to postharvest diseases of fruit and vegetables. *J. Sci. Food Agric.* **2021**, *101*, 1744–1757, doi:10.1002/jsfa.10829.

~~57~~55. Ragasova, L.; Penazova, E.; Gazdik, F.; Pecenka, J.; Cechova, J.; Pokluda, R.; Baranek, M.; Grzebelus, D.; Eichmeier, A. The change of bacterial spectrum after storage of X. campestris pv. campestris inoculated cabbage heads (Brassica oleracea var. capitata L.). *Agronomy* **2020**, *10*, 443, doi:10.3390/agronomy10030443.

~~58~~56. Erdrich, S.H.; Sharma, V.; Schurr, U.; Arsova, B.; Frunzke, J. Isolation of novel Xanthomonas phages infecting the plant pathogens X. translucens and X. campestris. *Viruses* **2022**, *14*, 1449, doi:10.3390/v14071449.

~~59~~57. Rossignol, G.; Merieau, A.; Guerillon, J.; Veron, W.; Lesouhaitier, O.; Feuilloley, M.G.; Orange, N. Involvement of a phospholipase C in the hemolytic activity of a clinical strain of Pseudomonas fluorescens. *BMC Microbiology* **2008**, *8*, 189, doi:10.1186/1471-2180-8-189.

~~60~~58. Yong, L.X.; Calautit, J.K. A Comprehensive review on the integration of antimicrobial technologies onto various surfaces of the built environment. *Sustainability* **2023**, *15*, 3394, doi:10.3390/su15043394.

~~61~~59. Taheri, P.; Soweyzi, M.; Tarighi, S. Application of essential oils to control some important fungi and bacteria pathogenic on cereals. *J. Nat. Pesticide Res.* **2023**, 100029, doi:10.1016/j.napere.2023.100029.

~~62~~60. Bournonville, L.; Askri, D.; Arafah, K.; Voisin, S.N.; Bocquet, M.; Bulet, P. Unraveling the Bombus terrestris hemolymph, an indicator of the immune response to microbial infections, through complementary mass spectrometry approaches. *Int. J. Mol. Sci.* **2023**, *24*, 4658, doi:10.3390/ijms24054658.

~~63~~61. Mousa, S.; Magdy, M.; Xiong, D.; Nyaruabaa, R.; Rizk, S.M.; Yu, J.; Wei, H. Microbial profiling of potato-associated rhizosphere bacteria under bacteriophage therapy. *Antibiotics* **2022**, *11*, 1117, doi:10.3390/antibiotics11081117.

~~64~~62. Jia, Y.; Zhao, L. The antibacterial activity of fluoroquinolone derivatives: An update (2018–2021). *Eur. J. Med. Chem.* **2021**, *224*, 113741, doi:10.1016/j.ejmech.2021.113741.

~~65~~63. Jiang, S.; Yang, G.; Shi, L.; Fan, L.; Pan, Z.; Wang, C.; Chang, X.; Zhou, B.; Xu, M.; Wu, L.; Xu, C. Design, Catalyst-Free Synthesis of New Novel α-Trifluoromethylated Tertiary Alcohols Bearing Coumarins as Potential Antifungal Agents. *Molecules* **2023**, *28*, 260, doi:10.3390/molecules28010260.

~~66~~64. Zhou, B., Yuan, X., Fan, L., Pan, Z., Chang, X., Jiang, S., Wu, L., Wang, C., Yang, G., Ji, X., Shi, L., Xu, C. Synthesis and antifungal activities of novel trifluoroethane derivatives with coumarin, indole and thiophene. *J. Saudi Chem. Soc*. **2022**, *26*, 101572, doi:10.1016/j.jscs.2022.101572.

~~67~~65. Ray, M.; Ray, A.; Dash, S.; Mishra, A.; Achary, K.G.; Nayak, S.; Singh, S. Fungal disease detection in plants: Traditional assays, novel diagnostic techniques and biosensors. *Biosens. Bioelectron.* **2017**, *87*, 708–723, doi:10.1016/j.bios.2016.09.032.

~~68~~66. Wang, T.; Gao, C.; Cheng, Y.; Li, Z.; Chen, J.; Guo, L.; Xu, J. Molecular diagnostics and detection of oomycetes on fiber crops. *Plants* **2020**, *9*, 769, doi:10.3390/plants9060769.

~~69~~67. Mastanjevic, K.; Krstanovic V.; Mastanjevic, K.; Sarkanj, B. Malting and brewing industries encounter *Fusarium spp*. related problems. *Fermentation* **2018**, *4*, 3, doi:10.3390/fermentation4010003.

~~70~~68. Yu, H.; Yang, H.; Haridas, S.; Hayes, R.D.; Lynch, H.; Andersen, S.; Newman, M.; Li, G.; Martínez-Soto, D.; Milo-Cochavi, S.; Hazal Ayhan, D.; Zhang, Y.; Grigoriev, I.V.; Ma, L.-J. Conservation and expansion of transcriptional factor repertoire in the *Fusarium oxysporum* species complex. *J. Fungi* **2023**, *9*, 359, doi:10.3390/jof9030359.

~~71~~69. Han, J.-H.; Park, G.-C.; Kim, K.S. Antagonistic evaluation of Chromobacterium sp. JH7 for biological control of ginseng root rot caused by *Cylindrocarpon* destructans. *Mycobiology* **2017**, *45*, 370–378, doi:10.5941/MYCO.2017.45.4.370.

~~72~~70. Shi, Y., Si, H., Wang, P., Chen, S., Shang, S., Song, Z., Wang, Z., Liao, S. Derivatization of natural compound β-pinene enhances its in vitro antifungal activity against plant pathogens. *Molecules* **2019**, *24*, 3144, doi:10.3390/molecules24173144.

~~73~~71. Wang, L.; Wang, N.; Yu, J.; Wu, J.; Liu, H.; Lin, K.; Zhang, Y. Identification of Pathogens Causing Alfalfa Fusarium Root Rot in Inner Mongolia, China. *Agronomy* **2023**, *13*, 456, doi:10.3390/agronomy13020456.

~~74~~72. Chudinova, E.M.; Platonov, V.A.; Alexandrova, A.V.; Elansky, S.N. Biology and resistance of phytopathogenic fungus Ilyonectria crassa to fungicides. *Plant Protect. News* **2020**, *103*, 192–196, doi:10.31993/2308-6459-2020-103-3-13431.

~~75~~73. Dubovoy, V.; Nawrocki, S.; Verma, G.; Wojtas, L.; Desai, P.; Al-Tameemi, H.; Brinzari, T.V.; Stranick, M.; Chen, D.; Xu, S.; Ma, S.; Boyd, J.M.; Asefa, T.; Pan, L. Synthesis, characterization, and investigation of the antimicrobial activity of cetylpyridinium tetrachlorozincate. *ACS Omega* **2020**, *5*, 10359–10365, doi:10.1021/acsomega.0c00131.

~~76~~74. Ardizzoni, A.; Pericolini, E.; Paulone, S.; Orsi, C.F.; Castagnoli, A.; Oliva, I.; Strozzi, E.; Blasi, E. In vitro effects of commercial mouthwashes on several virulence traits of *Candida albicans*, *viridans streptococci* and *Enterococcus faecalis* colonizing the oral cavity. *PLoS One* **2018**, *13*, e0207262, doi:10.1371/journal.pone.0207262.

~~77~~75. Araujo, H.C.; Arias, L.S.; Caldeirão, A.C.M.; Assumpção, L.C.d.F.; Morceli, M.G.; de Souza Neto, F.N.; de Camargo, E.R.; Oliveira, S.H.P.; Pessan, J.P.; Monteiro, D.R. Novel colloidal nanocarrier of cetylpyridinium chloride: Antifungal activities on Candida species and cytotoxic potential on murine fibroblasts. *J. Fungi* **2020**, *6*, 218. doi:10.3390/jof6040218.

~~78~~76. Pane, C.; Caputo, M.; Francese, G.; Manganiello, G.; Lo Scalzo, R.; Mennella, G.; Zaccardelli, M. Managing Rhizoctonia damping-off of rocket (Eruca sativa) seedlings by drench application of bioactive potato leaf phytochemical extracts. *Biology* **2020**, *9*, 270, doi:10.3390/biology9090270.

~~79~~77. Moreno-Gavira, A.; Dianez,F.; Sanchez-Montesinos, B., Santos, M. Biocontrol Effects of *Paecilomyces variotii* against fungal plant diseases. *J. Fungi* **2021**, *7*, 415, doi:10.3390/jof7060415.

~~80~~78. APEX2 Version 2.1), SAINTPlus. Data Reduction and Correction Program Version 7.31A, Bruker Advansed X-ray Solutions, BrukerAXS Inc., Madison, Wisconsin, USA, 2006.

~~81~~79. Sheldrik, G.M. SADABS, Program for empirical X-ray absorption correction, Bruker-Nonis, 1990 - 2004.

~~82~~80. Sheldrick, G.M. A short history of SHELX. *Acta Crystallogr., Sect. C: Struct. Chem.* **2015**, *71*, 3, doi:10.1107/S2053229614024218.

~~83.~~81. Präbst, K.; Engelhardt, H.; Ringgeler, S.; Hübner, H. Basic Colorimetric Proliferation Assays: MTT, WST, and Resazurin. *Methods Mol. Biol.* **2017**, *1601*, 1–17, doi:10.1007/978-1-4939-6960-9_1.

82. AAT Bioquest, Inc. (2022, March 17). Quest Graph™ IC50 Calculator. AAT Bioquest.

83. Ayoup, M.; Wahby,Y.; Abdel-Hamid, H.; Ramadan, E.; Teleb, M.; Abu-Serie, M.; Noby, A. Design, synthesis and biological evaluation of novel a-acyloxy carboxamides via Passerini reaction as caspase 3/7 activators. *Eur. J. Med. Chem.* **2019**, *168*, 340-356, doi:10.1016/j.ejmech.2019.02.051.

84. Born, G. Aggregation of blood platelets by adenosine diphosphate and its reversal. *Nature* **1962**, *194*, 927-929, doi:10.1038/194927b0.